Guitar playing and electromyoneurography:

Recording and sonifying the motor interaction of the guitarist's strumming hand using nerve EEG.

Master Thesis

Thomas Michael Wilmot

AALBORG UNIVERSITY

23/04/2018

Application for Thesis Contract

Type of thesis
Master's Thesis (kandidatspeciale / afgangsprojekt)

Student(s)

Name	CPR no.	Email
Thomas Michael Wilmot	260693-3811	twilmo14@student.aau.dk

T. Wilmot

Signature

School and Study Board
School of Information and Communication Technology (SICT)
Studienævn for Medieteknologi

Programme
Sound and Music

Project Supervisor(s)
Sofia Dahl <sof@create.aau.dk> Signature

Hendrik Purwins <hpu@create.aau.dk> Signature

Project Title
Guitar playing and electromyoneurography: Recording and sonifying the motor inte raction of the guitarists strumming hand using nerve EEG

Starting	Deadline	ECTS Credits
01/09	30/06/2018	30

Project Description
For my thesis I wish to continue the work on Nerve EEG from previous semesters, 8 and 9. The primary goal of my master thesis is to validate Nerve EEG as a technique for recording motor interaction during guitar playing. When applied to guitar playing movements, this technique indicates when note onsets will occur, the force going to be applied to the strings and the directness or smoothness in motion prior to and during a strum motion. The next stage is to take the separated motor components that are combined to strum a guitar and classify them per muscle movement. Then sonifying details of these movements, such as force applied and motion smoothness, by augmenting the original guitar audio.

Covering movement analysis techniques learned from Embodied Interaction. Utilising machine learning and source separation techniques learned from Multivariate Statistics and Signal Analysis. Also building upon audio processing techniques learned throughout this masters course. The validation of Nerve EEG technique will have implications that reach beyond understanding musicians movements. It could help understanding how our senses and movements are communicated using analogue signals in the body, which could be used to improve cochlear implants for example.

Plan for Thesis Supervision and Lab Work

The thesis supervisor meets with the student(s) approximately once a week to discuss progress, time schedule, resources, lab work, ideas, issues etc.

Approved by Head of Studies

3/5-2018

Date

Signature

(This page is intentionally blank.)

Contents

Chapter 1
Guitar Interaction

1.1 Introduction

With over seventy years of technological innovation, the electric guitar with its accompanying amplifiers and sound processing units, also known as ‘effects’, represents the sole example of an electroacoustic instrument where the link between instrumental gestures and audio can be experienced across multiple musical contexts (O.Lähdeoja, 2010). Moving from acoustic to electric guitar had a massive influence in western popular music culture; challenging the concepts of what is noise or musical sound (S.Waksman, 1999). Though innovation of the guitar continues through interaction with digital technologies, developments are typically grounded in the instrument’s ‘cultural identity’, referring to the ways the guitar is used to challenge and influence music culture (G.Carfoot, 2006). This is prominent in the lack of dynamic interaction with the augmented features of the instrument, characterised by a monolithic use of timbres, selected by on/off effectors which remain musically static (O.Lähdeoja, 2010).

1.2 Guitar Effects and Interaction

“Guitar distortion is a particularly powerful expressive device, evoking abrasiveness and emotional instability; it can even act as a kind of timbral leitmotif for ideas expressed in the lyrics.”- Thompson (2015)

Being able to augment the timbre of the guitar is a tool with currently untapped potential due to the fact current effects are designed based on the system of the electric guitar and its connected switches. The aim of this thesis is to investigate the possibility of using motion and force applied by muscles as source of control for guitar effects. Designing around the user and their strumming interaction with the guitar.

Chapter 2

From thought to motion

This chapter covers how to record and extract data from the motor interaction of the guitarist's strumming hand during performance. Starting with a brief introduction to how motion commands are conducted through the body. The basics of recording those commands as electrical signals from the muscles and nerves. The decoding of those electrical signals is investigated with a comparison of decomposition methods. Lastly, the author proposes a method for extracting the data for multiple muscles via recording their shared nerves for the purpose of tracking the guitarist's interaction of the strumming hand.

2.1 Signal Chain

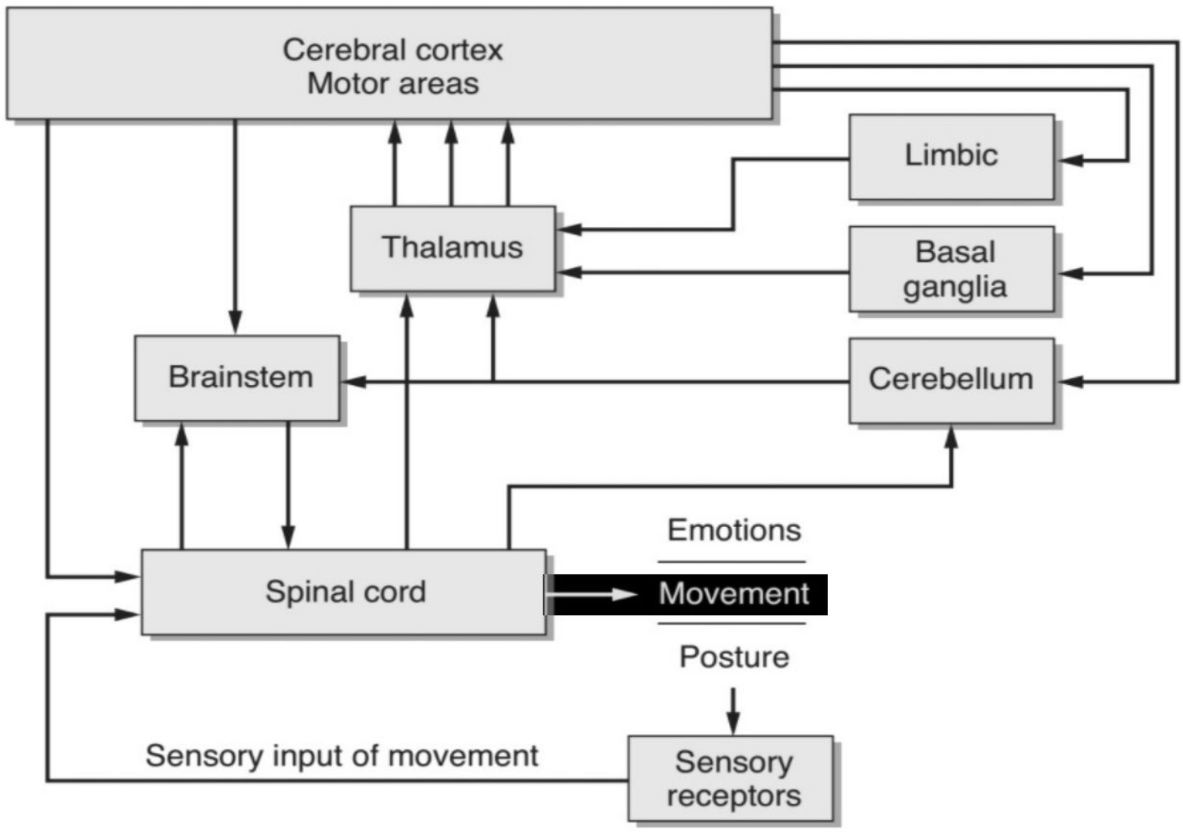

(Fig 1. Nervous System Control. Image from: (E.Criswell, 2010). Cram's introduction to surface electromyography.)

Voluntary motions begin as a series of electric sparks in the brain. These sparks are known as *'action potentials'* or *'spikes'* (Gerstner,2014). They are conducted through the body via cells called *'neurons'*. The spikes then reach the desired muscle, which is the combination of a bundles of strand like fibers controlled by motor neurons called *'motor units'*. Those motor units may then cause movement by varying their tension or length, depending on the incoming spikes (Cram, 2011).

2.2 Neurons

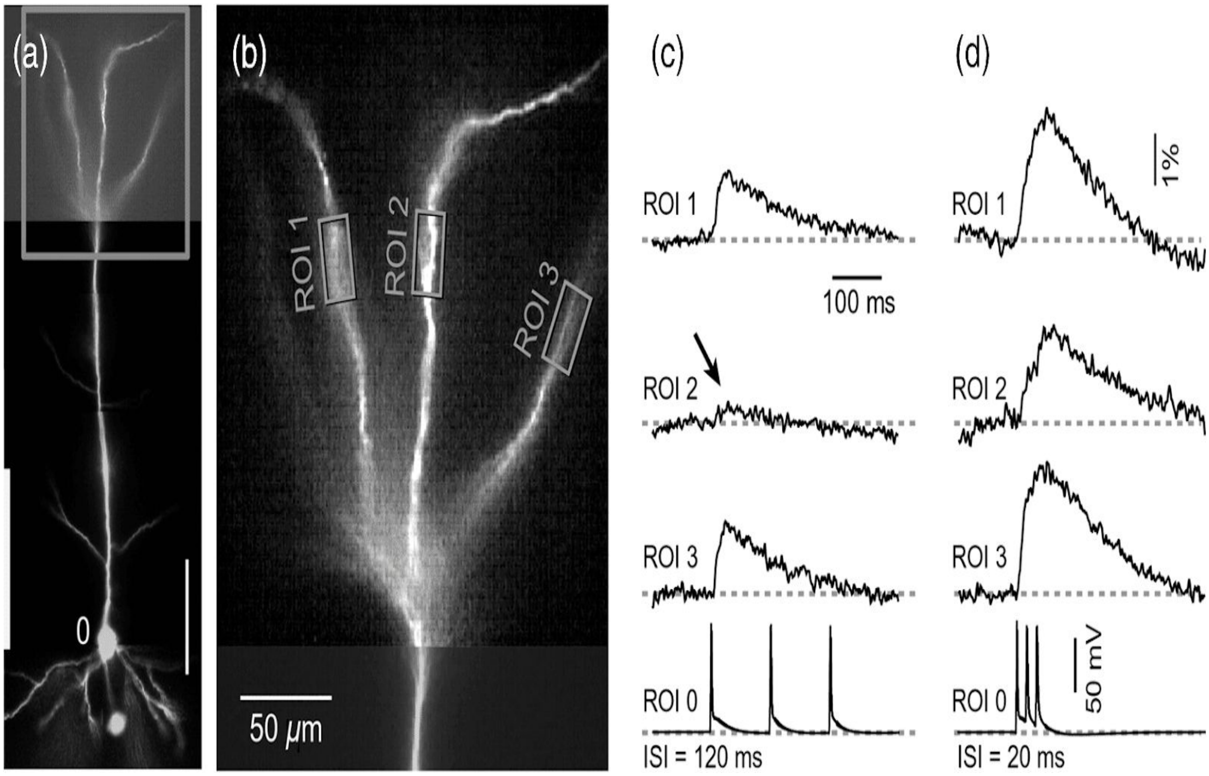

(Fig 2. (a) Neuron (b) Dendrites (c) 120ms ISI input results (d) 20ms ISI input results. Image from Branch specific... (Wen-Liang Zhou et al. 2014).)

Above, in figure 2 part (a), is a photo of a neuron. At point 0 in (a) is the *'soma'*. The soma generates spikes when stimulated, above a voltage-threshold, either by combining the output of prior neurons carrying spikes or artificially using an electrode (Gerstner, 2014). Spikes are then conducted via the longest part of the neuron, the *'axon'*. At the end of the neuron are branches known as *'dendrites'*, shown more clearly in figure 2 part (b). Dendrites, much like the soma, act like capacitors so conduct a spike only once a voltage-threshold is reached. Spikes may then arc from a dendrite to the soma of the next closest neuron (Gerstner, 2014).

2.3 Nerves

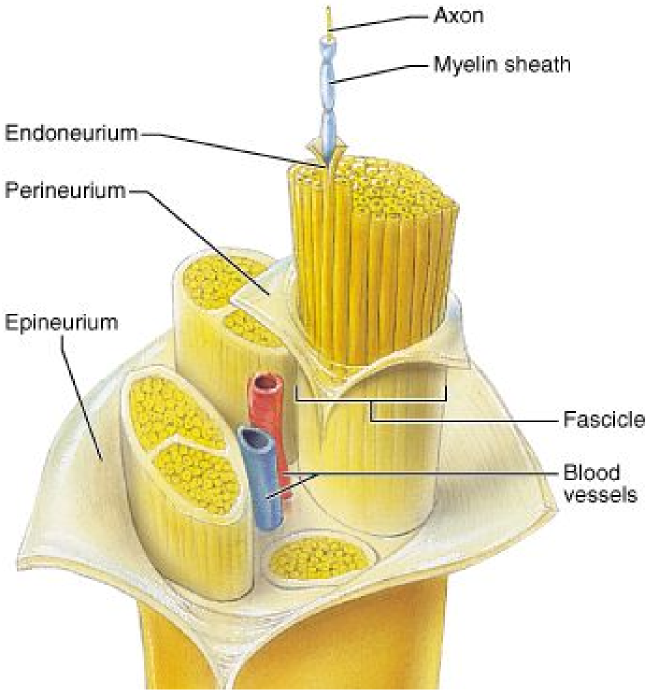

(Fig 3. Nerve Cross Section, Wikipedia)

Aligned consecutively, neurons form nerves. Figure 3, above, is a cross section diagram of a nerve. In this example, it shows the axon is covered in a *'myelin-sheath'*. This is an electric insulator that helps conduct spikes along the axon faster and reduces signal loss and interference (Purves, 2001). Worth noting from this diagram is that several neurons are bundled together in close proximity.

2.4 Action Potentials (Spikes)

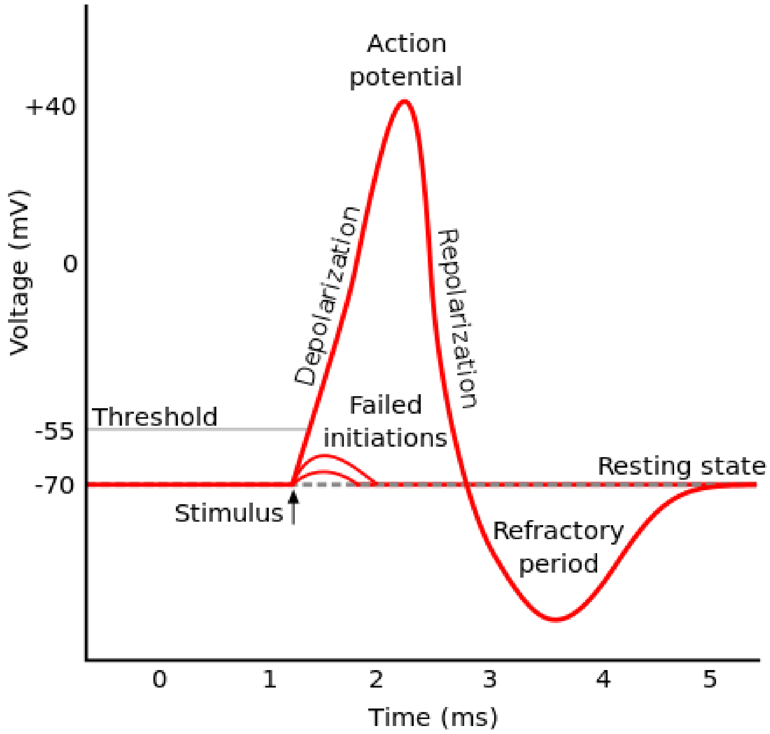

(Figure 4, Action potential schematic, Wikipedia.)

After being fired from somas and passed through dendrites, action potentials or spikes have a unique shape per neuron (Gerstner, 2014). For the purpose of extraction from recordings, the ideal action potential or spike (shown above in figure 4) can be described thus:

A neuron may generate a spike or fails to fire, dependant on the strength or rate of the incoming stimulus. Weak or low rate stimuli appear as failed initiations. When fired, the spike is characterised by a period of depolarisation, rising 110mV from the neuron's resting voltage potential of -70mV, and repolarisation, dropping to -90mV, lasting 1 to 2 ms. Followed by a refractory period where the neuron cannot fire again until it returns to its resting state at -70mV.

2.5 Recording Action Potentials

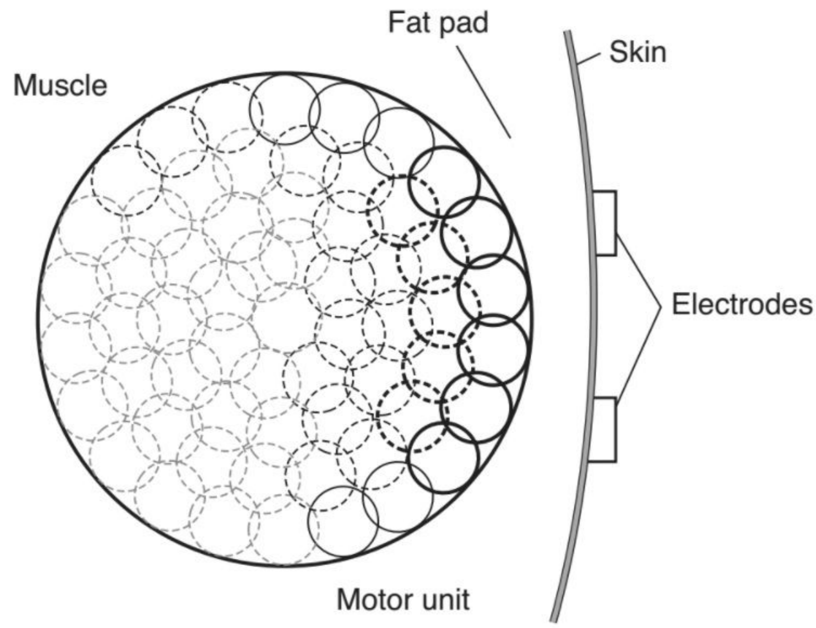

(Fig 5. Recording area. Image from: (E.Criswell, 2010). *Cram's introduction to surface electromyography*.)

The title *'electromyoneurography'* (MB.Spiegel, 1978) refers to the combination of simultaneously recording spikes at motor units (electromyography, EMG) and neurons in the nerve or brain (electroneurography, ENG).

EMG surface recordings are typically done using paired surface electrodes, placed on the skin over muscle (as shown in figure 5, above). The motor units that combine to form the muscle may vary their tension and length when activated. However, much like rubber bands, motor units may snap if under too much strain. Therefore, the greater the strain the muscle is under, the more motor units are activated or 'recruited' at a firing rate between 8 and 50Hz, rotating the load between motor units (E.Criwell, 2010). On recordings, the increase in motor unit firing activity is shown as an increase in RMS-voltage (the average voltage over time within a set window).

ENG recordings are not typically done using surface electrodes over nerves due to the myelination of the nerve neurons. Myelin insulates the electric signal resulting in low signal-to-noise ratio ('SNR' henceforth) in recordings. Therefore, ENG recordings are normally performed using needle electrodes injected in close proximity to the target neurons. This is also known as an *'in-vivo'* recording. For in-vivo recordings, raw data is typically has a high SNR. Thus require little noise reduction processing other than averaging over several trials and spikes are detected using a simple threshold detector (Choi, 2006. Gerstner, 2014.).

2.6 Encoding motion with spike-trains

When a neuron fires a sequence of spikes at semi-regular intervals, due to a stimulus or motion command, the collective sequence is called a '*spike-train*'. Stimulus, in the case of guitar strumming refers to the specific motion to be performed and the intensity which the muscles used must contract. The more intense or effective the stimulus, the higher the rate of spikes. Consistent rate codes in spike trains and the spike-stimuli phase relationship may afford stimulus recognition and reconstruction.

Describing surface recordings of spike-trains as highly irregular and if sonified would resemble noise; Gerstner (2014) states that determining whether said noise is highly efficiently encoded information or meaningless flicker is one of the most burning problems in neuroscience. Therefore, Gerstner (2014) uses either simulated models of idealistic spike-trains or in-vitro recordings (isolated neurons in glass recorded by inserting a multi-electrode needle into the tissue in close proximity to the cells) which utilise artificial stimulation, so the stimuli can be controlled and the neurons react in a reliable way. These allow him to better demonstrate techniques for reducing the complexity of neuron models or extracting information about how the neurons react to the designed input stimuli. However, Gerstner (2014) does highlight a method, called *'Peri-Stimulus-Time Histogram'* (PSTH henceforth), that can extract near consistent spike-trains of multiple neurons from surface recordings.

The rate coding later used to determine the onset, offset and intensity of a muscle contraction can be estimated using the PSTH, shown below in figure 6, where spikes are illustrated by solid vertical lines. Conducted by recording the activity of a neuron to a repeated stimuli over several trials or 'runs'. The probability of a spike firing (*p*) per time window (Δt) is calculated by averaging over the several recordings aligned in synchronicity with the stimuli. For guitar strumming, this would be from when the motion of strumming begins until the motion is stopped or changes direction; causing a different new motion and different set of muscles to initiate. Randomly firing spikes and areas of noise are removed by applying a threshold gate to the output of the PSTH. Then the most probable rate code of the spike train may be extracted by finding the peaks of the threshold filtered PSTH. Combining the rate coding and the phase relation of spikes to each stimuli (*'phase coding'*) for each motion can be used to identify which muscle the neuron is innervating and how much force that muscle will apply (Gerstner, 2014).

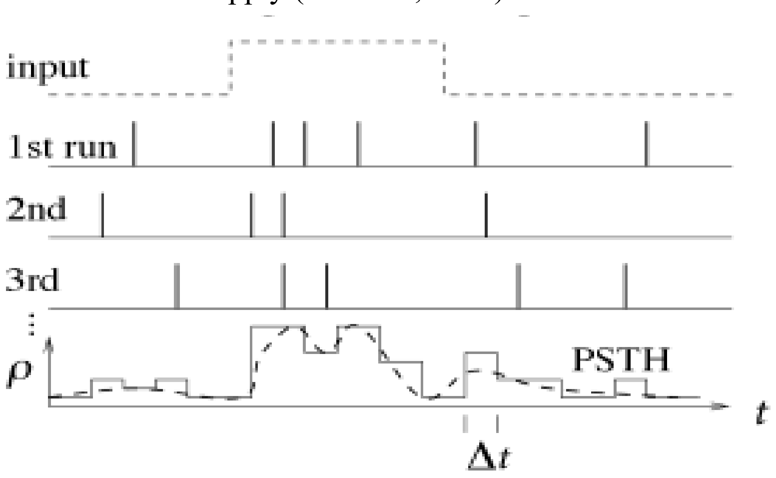

(figure 6, Peri-Stimulus-Time Histogram PSTH (W.Gerstner, 2014))

2.7 Approaches for EMG/ENG Decomposition

Surface recordings of nerves by definition are composed from the firing activity of multiple neurons. So when PSTH is applied to raw data, the overlapping spike trains of the multiple neurons create a continuous level of probability of spike firing. Meaning the rate codes that identify each muscle motion and intensity are lost in the noise of the surrounding neurons. The surrounding neurons may also be carrying spike trains for other motions and muscles but more often it is the sensory feedback from the motion itself. Therefore, to isolate spike trains that determine motor interaction, first the spikes have to be sorted per their generative neuron.

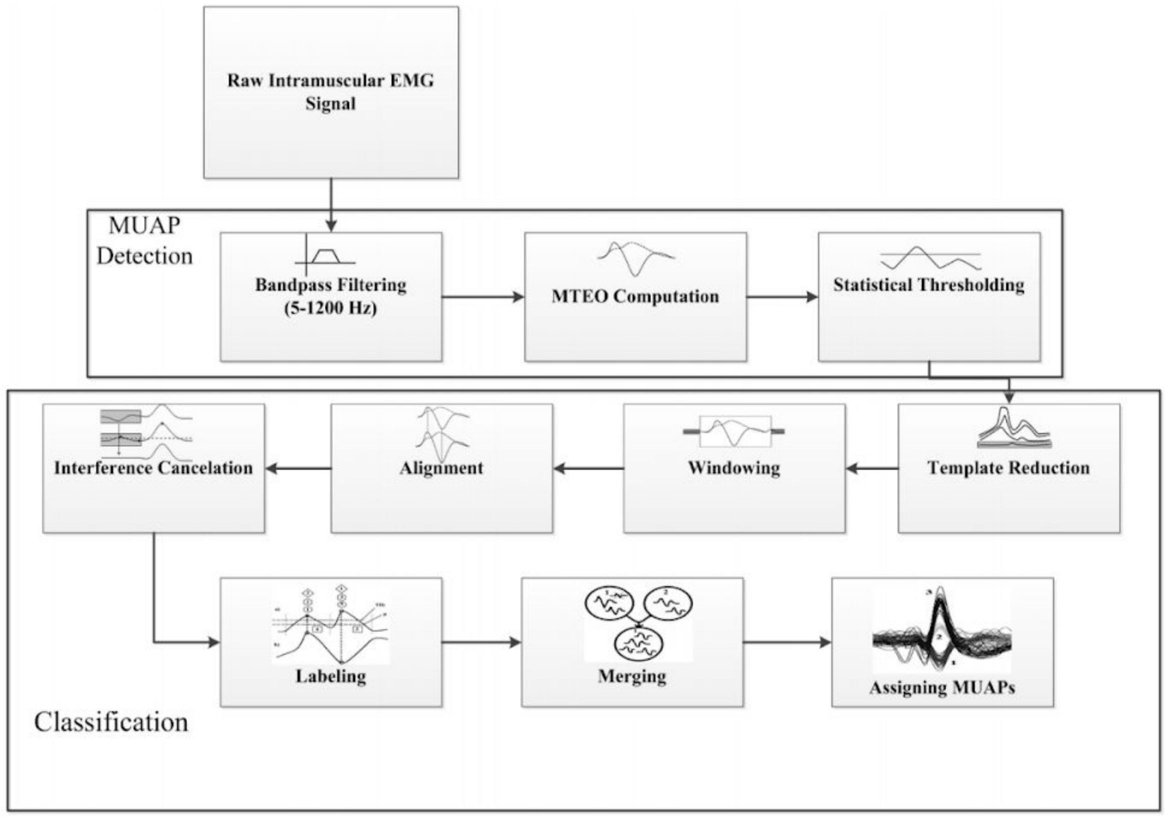

(Fig 7 . Raw signal Input, MUAP Detection and Classification. Sedghamiz 2015)

Sedghamiz (2015) separates the processes of EMG/ENG demoposition into two stages; 1: detection and 2: classification. Franke (2015) similarly describes it but as three stages of *'spike sorting'*; 1: detection of spikes, 2: estimation of the number of neurons and their templates and, lastly, 3: assigning individual spikes to their neuron. These three steps must be iterated to solve the three major problems that exist within detection and classification of spikes; alignment, threshold detection level and superposition resolution.

Spike alignment refers to the process where the timing of a detected spike is determined. With high SNR signals, spikes may be aligned according to global extrema, positive or negative peaks or by their threshold crossing points. However, in low SNR signals, noise and superimposed spikes may cause the the spike shape to be deformed. Misalignment can lead to classification errors. Choi (2006) demonstrates this in figure 8 (below). The two detected spikes shown in (a), *S* and *S'*, were identical until deformed by noise. Aligning by global extrema, shown in (b), causes misalignment and classifies the spikes wrongly to different neurons.

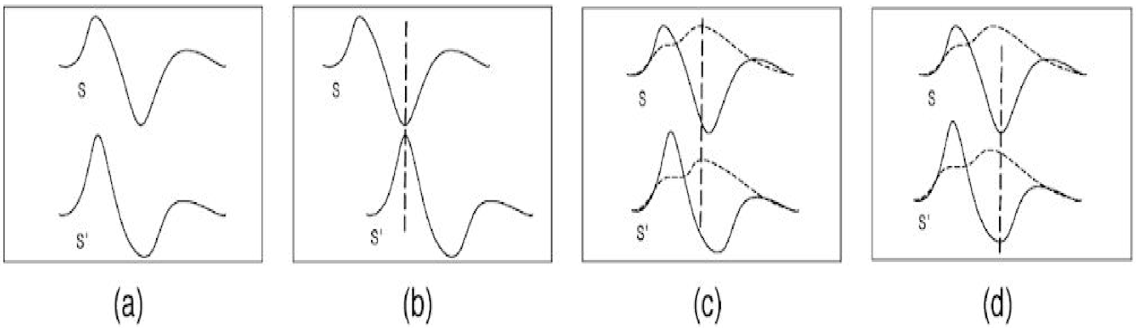

Alignment methods. (a) Deformed segments. (b) Global extremum alignment. (c) MTEO alignment (STEP I). (d) MTEO alignment (STEP II).

(Fig 8. Alignment methods. Image from Choi 2006)

To achieve correct alignment, Sedghamiz follows Choi's two step method shown in (c) and (d), above. Where the global maximum of the mTeo output (curved dotted lines) is used to align the spikes initially, (c). Then the nearest extremum of the original signal to global maximum of the mTeo output become the reference points for alignment, (d).

MTeo is the method used by Sedghamiz (2015) and Choi (2006) which works well with low SNR signals. MTeo stands for *'Multi-resolution Teager energy operator'*, which is a time-frequency analysis method that can be tuned to be more sensitive to frequency bandwidths determined by the spikes. The instantaneous frequency characteristic of spikes makes this an effective method for detection and tool for alignment. MTeo works by calculating the instantaneous energy of the signal within a smoothing hamming window. Since MTeo is more sensitive to lower frequencies, a high pass filter is normally used.

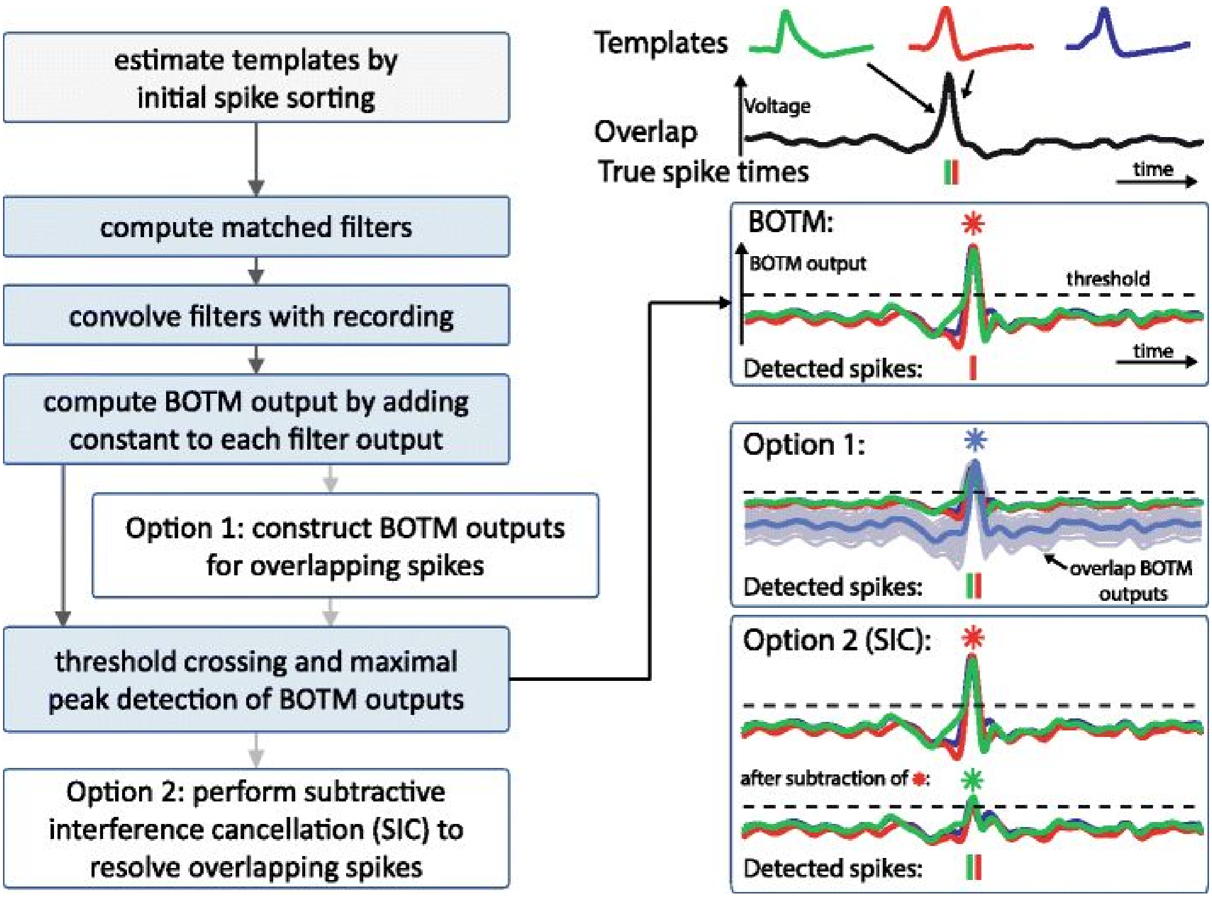

(Fig 9. Bayes Optimal Template Matching with Subtractive interference cancellation, Franke 2015)

Franke (2015) proposes a method called *'Bayes Optimal Template Matching'* (BOTM henceforth). This method assumes that the expected spike shapes are known and that the noise has a gaussian distribution. Unfortunately this means the method can only be applied in simulated conditions. This method is however highly effective and efficient at aligning spikes, especially in the case of two superimposed spikes.

Above in figure 9 is a diagram of the BOTM method. Firstly, using templates of expected spike shapes, finite-impulse response (FIR) filters are created per neuron. These filters are adjusted so that the SNR is maximised for the spike shape with the gaussian noise for comparison. This is process is called *'Matched Filtering'* (Van Trees, 2002). The matched filters are convolved with the raw input data. BOTM is then computed with the matched filter outputs, giving the discriminant functions per filter that best separates clusters per neuron which share the same covariance matrix. Similar to linear discriminant analysis (LDA) (Fisher, 1936). Then the second major problem with spike detection and classification may be addressed.

Threshold detection level in simple data refers to the threshold which below is noise and above is a spike belonging to a particular neuron. Although, this can also refer to the threshold level that determines which neuron a spike belongs to. High SNR signals may utilise simple methods such as amplitude thresholding for spike detection; where the threshold level may adapt automatically based on the estimated noise level for example. Low SNR signals require more robust methods. Nenadic (2005) lists the most common detection methods for low SNR signals as; power or energy detection (Harris, 2000; Bankman, 1993), matched filtering (as described above), principal components (Bankman, 1993), Haar transformation (Yang, 1988) and the discrete-wavelet-packet transformation (Oweiss, 2002).

Franke (2015) applies an amplitude threshold detection level to all BOTM outputs, as shown in figure 9 above. Using the maximum between threshold crossings to mark the temporal instances of detected spikes.

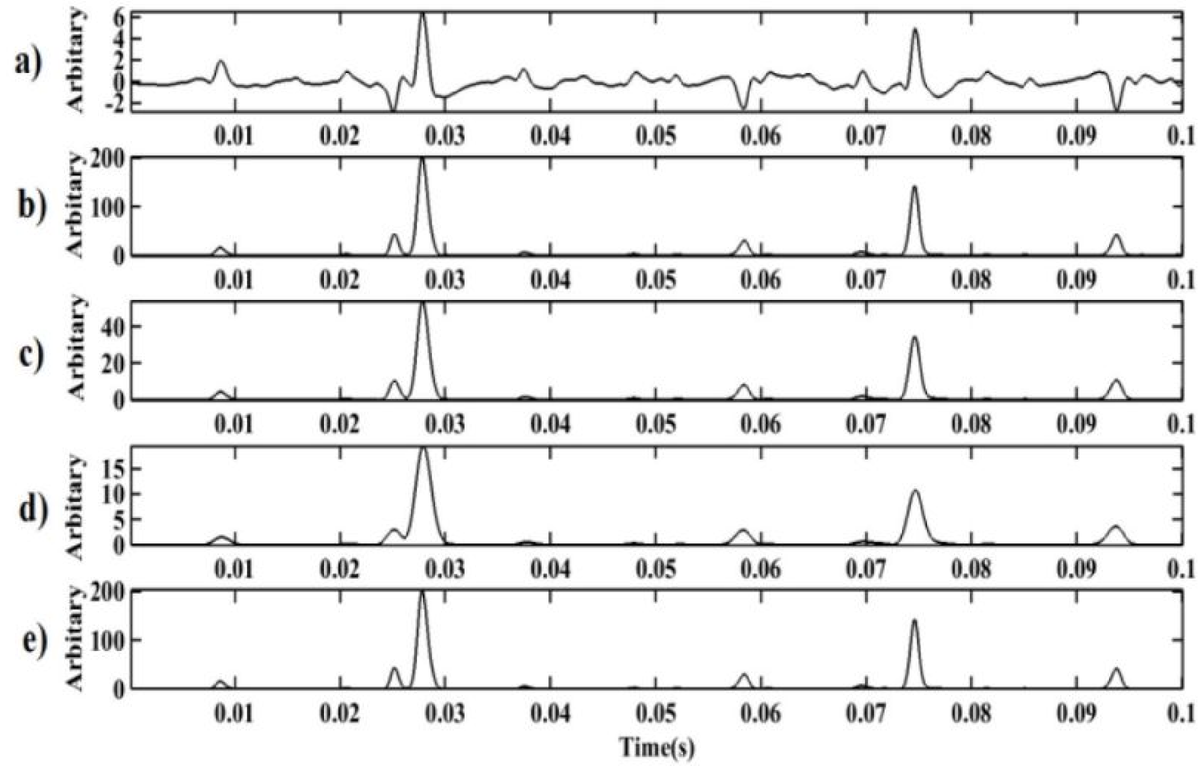

(Fig 10. (a) Band-pass filtered and normalised EMG signal. (b),(c) and (d) Outputs of k-Teo at k=2,3 and 5. Where 'k' is the lag parameter in MTeo. (e) MTeo output from maximum energy detector, Image from Sedghamiz (2015))

Sedghamiz (2015) uses a statistical thresholding similar to Nenadic (2005). Where for each resolution of k (shown above in figure 10) two states are calculated, first when there is only noise and the second state where there is a spike and noise. While Franke (2015) also uses bayesian hypothesis to sort spikes and determine their optimal discriminant functions, Sedghamiz (2015) differs by comparing the mean and standard deviation of the separated segments of spikes and noise at different scales; combining the outcomes from all scales to calculate the optimal threshold detection level. The scales are however set by the user manually and must be iteratively adjusted in order to optimise the sensitivity of the MTeo method to noise and spikes.

Superposition resolution is the problem that occurs when two or more spikes are superimposed on the same recording and are near simultaneous. Two methods are shown in figure Franke, 2015above; Option 1: Simulate the expected superimposed spike template from existing ones or Option 2: Subtractive interference cancellation (SIC). The latter is used by both Franke (2015) and Sedghamiz (2015). However, subtracting any signal from a noisy recording reduces the remaining signal below the detection threshold in most cases. As for simulating the superimposed spikes template with varying overlap, this can be very accurate for determining the timing of two superimposed spikes using the BOTM method. However, the fewer spike templates; the more error prone this technique is and can become computationally slow over long recordings (Franke, 2015).

2.8 Chapter Summary

The rate coded spike trains that determine which muscles are used and how intensely the muscles contract may be recorded using surface electrodes. The SNR for surface recordings of nerve neurons will be very low due to the myelination of the nerves. Therefore, averaging over several trials or an alternative method to PSTH must be applied create reliable spike train rate codes. It requires robust processing methods to separate the spike trains per their generative neuron in low SNR signals. MTeo will work best in this case but requires iterative manual adjusts to detection sensitivity. To test the validity of surface recordings of nerve neurons for muscle tracking, the motions performed should be initially simplified such that only one muscle is activated at any given time. The motion performed should be done in opposition to measurable forces such as weights to find if different forces applied by the same muscle can be identified. The same motion may be performed several times to enable averaging out noise spikes.

Chapter 3

Test and Processing of Data

3.1 Muscles, nerves, motion and electrode placement

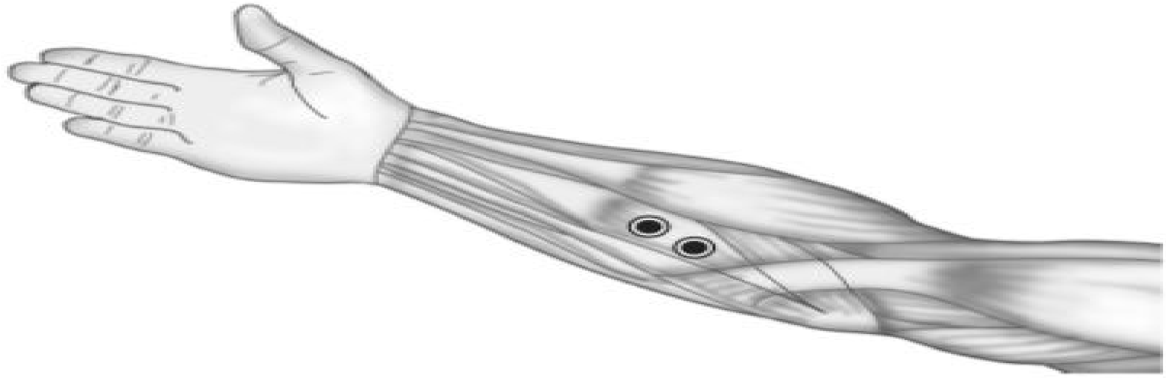

(fig 11. Electrode Placement for Muscle Group 1. Image from:Criswell, E. (2010). Cram's introduction to surface electromyography.)

Muscles: Flexor Carpi Radialis and Palmaris Longus

Motions: Wrist Flexion + Radial Deviation

Nerve: Median Nerve

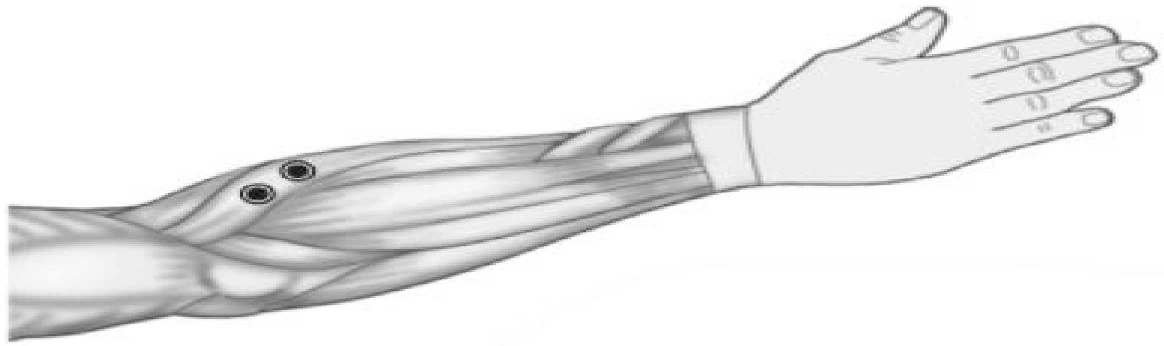

(fig 12. Electrode Placement for Muscle Group 2. Image from: Criswell, E. (2010). Cram's introduction to surface electromyography.)

Muscles: Extensor Carpi Radialis (Longus and Brevis)

Motion: Wrist Extension + Radial Deviation

Nerve: Radial Nerve

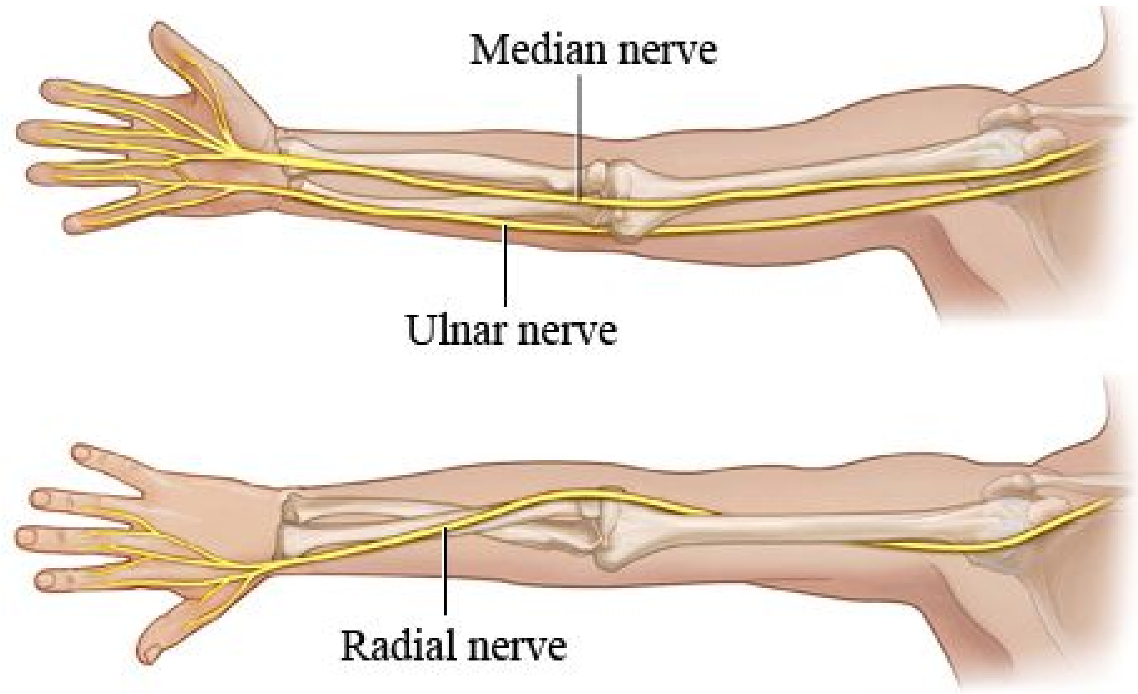

(fig 13. Nerves of the hand. Image from:
http://img.webmd.com/dtmcms/live/webmd/consumer_assets/site_images/media/medical/hw/h9991449_001.jpg)

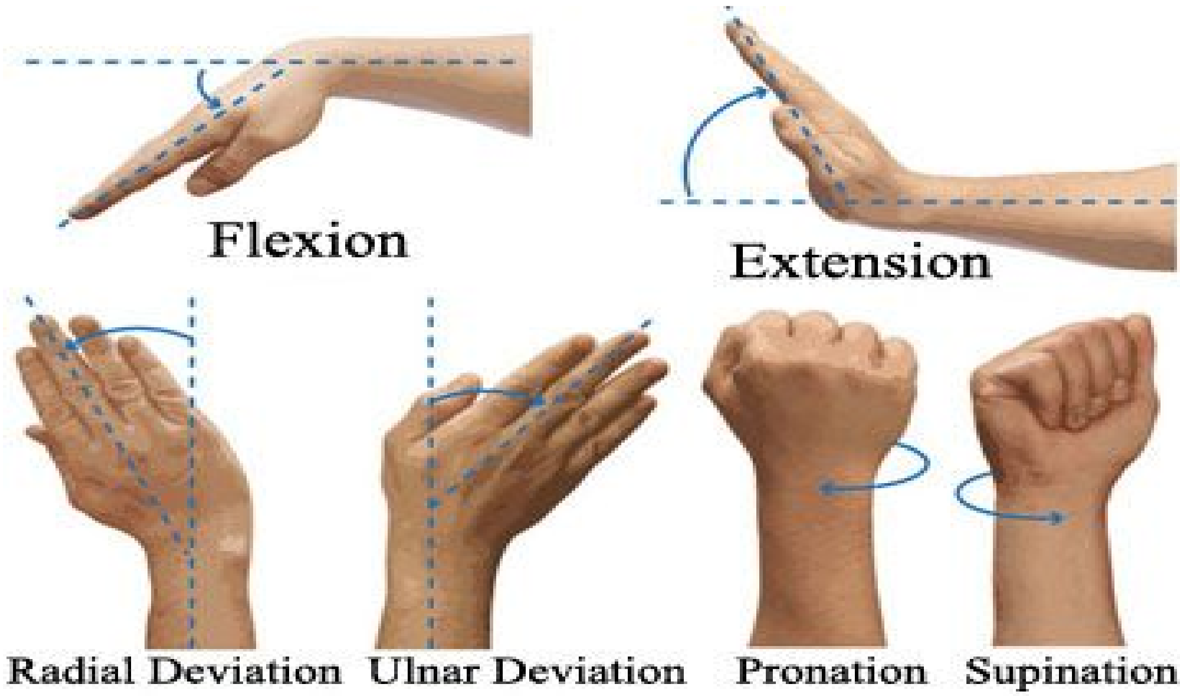

(fig 14. Hand-wrist motions. Image from: http://www.revolutionarytennis.com/Resourcess/wristandhandterm.jpeg)

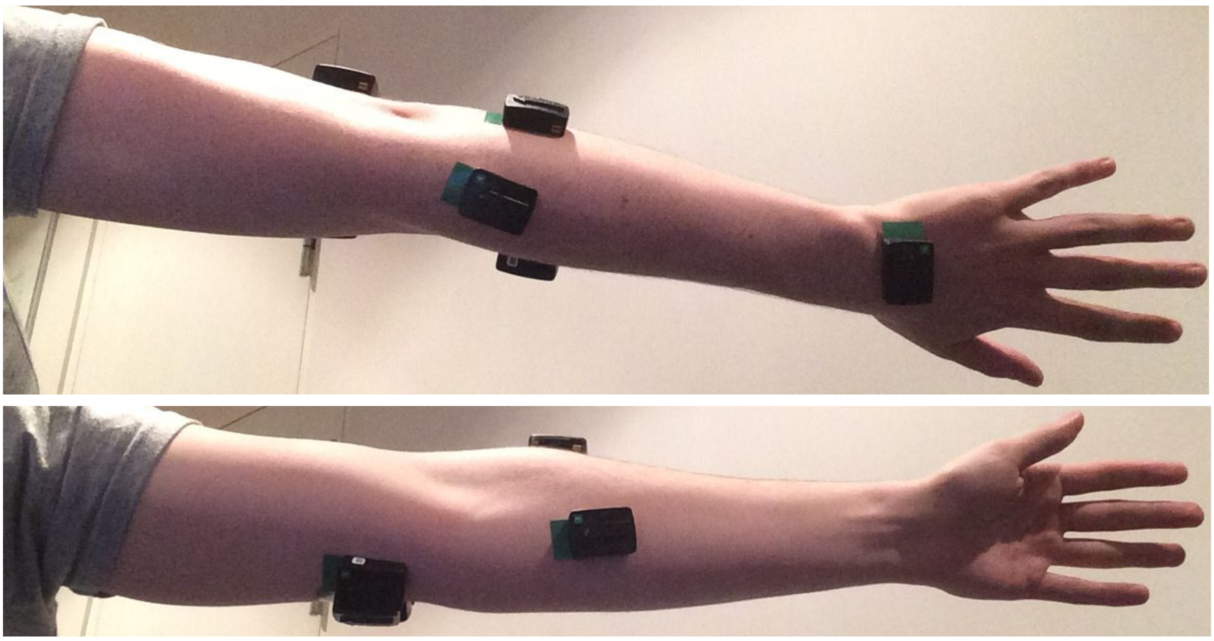

(Fig 15. Electrode placements for Nerve and muscles. Image by author 2018.)

3.2 Test Method

The motions radial deviation and wrist flexion (as shown in figure 14) were selected because the radial nerve (shown in figure 13) innervates both the flexor carpi radialis (‘FCR’) used for wrist flexion (muscle shown in figure 11) and extensor carpi radialis (‘ECR’) used for radial deviation (muscle shown in figure 12). Before applying the eight stick-on EMG/ENG electrodes shown in figure 15, the skin was rubbed clean with alcohol to reduce skin resistance which helps improve signal to noise ratio. Figures 11 and 12 were used as a starting point to find the correct placement of the electrodes. Then by performing the contractions and pushing against the muscle; the ‘belly’ or meatiest area of muscle was selected for the EMG sensors to get the strongest possible signal. The ENG (nerve) sensors were placed above the elbow in an array across the back of the arm where the radial nerve is most likely to pass through with the least amount of muscle which may interfere with the signal.

Separately motions ‘Radial Deviation’ and ‘Wrist Flexion’ were performed five times at increments of resistance by applied physical weights (small dumbbells attached with velcro straps to the hand) from no weight to 1kg and 2kg. Giving a total of thirty contractions with five total per six labels (*Labelled per motion and mass. ‘Radial Deviation 0kg’=1, ‘Radial Deviation 1Kg’=2, ’Radial Deviation 2kg’=3, ‘Wrist Flexion 0kg’=4,‘Wrist Flexion 1kg’=5,‘Wrist Flexion 2kg’=6.)*. The median duration of contractions was 2.5 seconds with a standard deviation of 0.6 seconds.

The arm was rested flat on the table to ensure auxiliary muscle activity would be minimised. Then recordings of 30 seconds were made per label. The contractions were held for their duration then a rest period equal to the length of contraction separated each contraction from the other. Each time the motion performed was changed or a new weight was to be attached, the recording would be stopped and a new one made. The time between recordings was kept to a minimum to reduce factors such as electrode to skin connection which may cause signal to noise ratio to degrade or fluctuate over time as the stick on electrodes lose grip.

The sensor used were the Delsys Trigno EMG surface electrode system (16). These sensors have motion tracking sensors such as 3 axis accelerometers as well as EMG electrodes with a sampling frequency of 1111.111Hz. Just high enough to be used for spike recordings. The system synchronises motion data from the sensor placed on the back of the hand with the recorded EMG and ENG data. The sensor placed on the back of the hand was used solely for motion tracking and synced with the other electrode sensors.

3.3 Processing of recorded data

(The code and data used for this project is available through the following github repository: https://github.com/twilmo14atgmaildotcom/ThomasMichaelWilmot_SMC10)

The raw data ENG and EMG data was passed through a highpass filter set to 300Hz. Then upsampled from 1111.11Hz to 2222.22Hz and smoothed with a lowpass filter set to

1000Hz. A notch filter at 50Hz was not required due to the electrodes using rechargeable batteries.

Labelled time windows were created from a combination of the motion tracking (3-axis accelerometer) and muscle activity (EMG) data. These are shown in Appendix B. The RMS voltage of the full wave rectified EMG data for the muscle being used gives the onsets and offsets of muscle activity. Similarly, a smoothing window is applied to the 3-axis accelerometer sensor giving hand position. The time windows mark when there is muscle activity and motion (contraction state, 1) and where there is no muscle activity or motion (resting state, 0).

To separate training and test data, these 30 contraction time windows were applied to the Nerve ENG data. Each contraction window was labelled per motion and mass attached to the hand. The indexing of test and training was done using k-fold cross-validation. Meaning for example, contraction 1of5 from label '(1)Radial Deviation 0kg' is used as test data; while contractions 2,3,4 and 5 are used as training. Then the next iteration, contraction 2of5 is test data and 1,3,4 and 5 are training data etc. This is to ensure that the results are true for all input data.

An adapted version of the Sedghamiz MTeo and statistical thresholding method described above in chapter 2 was applied to the filtered ENG data in Matlab to extract the spike firing times per neuron in the nerve. The weights 'spike threshold detection level' and 'similarity to spike template' used in the mTeo tool were adjusted to maximise the number of spike instances identified during the contraction states (true positives) and minimise spike instances identified in resting state (false positives). These weights initially required several manual adjustments and iterations before any reliable spike detection occurred. The weights were later adjusted automatically with a restricted range of known stable values in a loop comparing the precision (true positives/false positives+true positives) of spike detection against the expected correlation results per label(*described in more detail below*). The MTEO tool tended to be sensitive to high amplitude superimposed spikes or would wrongly identify noise as spikes.

Therefore, inspired by the BOTM method, I adjusted the statistical thresholding of the Sedghamiz method with aforementioned states; A. 'segment with noise' or B. 'segment with noise and spike'. Such that for case B, the statistical thresholding would identify the likelihood that the spikes were either independant or superimposed by amplitude threshold and then find the closest matching independant spike template generated by the MTeo method to the superimposed spikes using cross correlation. If there was a close match then the separated spikes and their timings would be added to their correct neuron. This resulted in accurate segments that matched the motion data and RMS-voltage of the EMG electrodes. So when there was a contraction and movement the segment would have several spikes and in areas where the arm was rested there were few to no spikes. From there the separated spikes per neuron could be investigated. This detected spikes per neuron and the contraction time windows can be seen in appendix C.

Across all data labels, the distributions of spike timings (the frequency of spike instances) were nearly identical. This was due to the inherent low SNR and sensory spike feedback (noise spike instances caused as a result of the contraction but not part of the motor command signal). A higher average rate could indicate increased muscle activity however; the same as with EMG. The method I used to try overcome this problem was to measure the interspike intervals between one spike and the next five spikes (shown in figure 16 below), creating ISI distributions per neuron. The range of interspike intervals was limited from the minimum time required before a neuron may fire again (refractory period 2-3ms) to the maximum set by the slowest motor unit recruitment rate of 8Hz (125ms). Distributions were then weighted according to the total spike instances per distribution to reduce the impact of low activity neurons later in analysis.

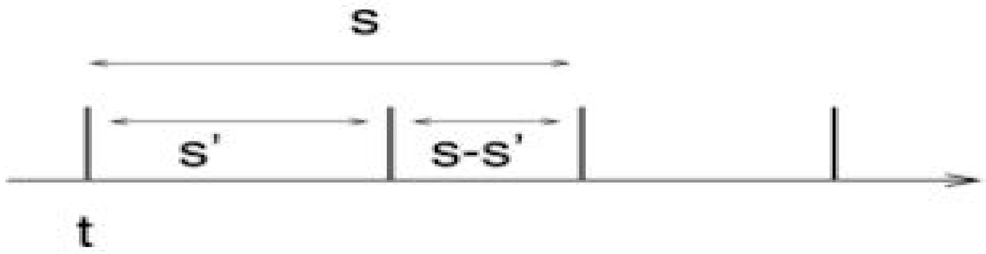

(figure 16. "The autocorrelation of a spike train describes the chance to find two spikes at a distance s, independent of the number of spikes that occur in between."-Gerstner 2014. Image from Gerstner,2014.)

Also known as the autocorrelation of a spike train. This method sums the ISI distributions with itself. Based on the theory that a neuron when presented with the same stimulus will react in the same way. Therefore over long data with a repeated and stable stimulus, this method may be used. However, in the case of my data, I used this method simply to reduce the impact of random spike timings (noise).

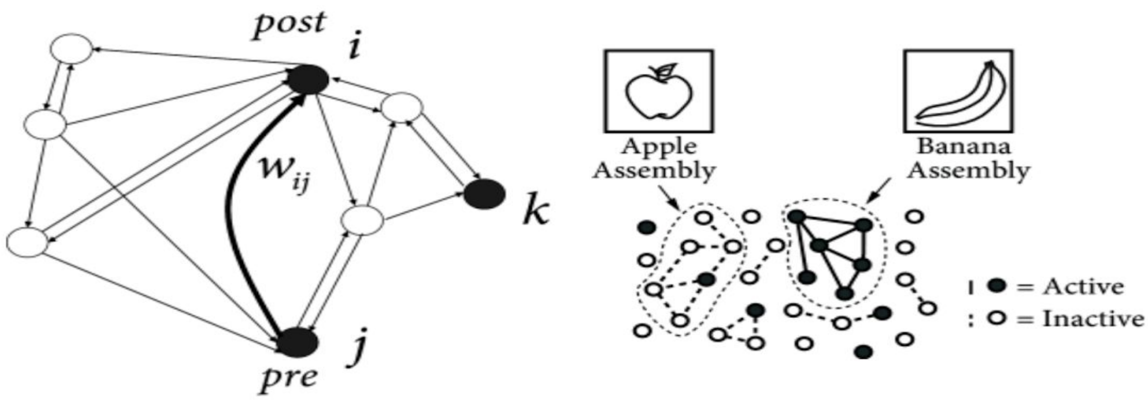

(figure 17. Neural network and Hebbians Theory. Image from Gerstner 2014.)

The second part of my trial method is based on Hebbian's theory (W.Gerstner, 2014). Which can be simplified into the phrase *"Neurons that fire together, wire together"*. This theory is used to describe the connections between neurons when firing and the impact that one neuron has on another. The higher the average firing rate of a neuron the more effect it has on the surrounding neurons. Therefore the neurons with similar ISI distributions and high average firing rates are more likely to be connected to and cause the muscle contractions. For the training data, I applied this by superimposing all ISI distributions based their correlation with the neuron with the most spikes. Similarly subtractive interference cancellation was used to subtract portions of ISI distributions that were the same across different labels which suggests common noise. The resulting ISI distributions for training and test data can be seen in appendix D.

Finally to test if the ISI distributions were related to the labels; so the ISI's could be used to classify nerve ENG data from contractions per motion performed and force applied; I performed cross correlation with the test data and training data using cross validation. The results are shown in Appendix E. Cross correlation was used because the duration and force applied in each contraction varied within recordings (shown in Appendix B, where a higher RMS value represents a higher force); I believed that force applied would result in a lateral shift of the ISI distribution and it would retain the same shape. To optimise the mTeo tool output (as previously mentioned above), check the correct ISI distribution range, effect of individual neurons and to extract the highest correlation results I applied a very simplified version of gradient descent. Where the weights 'detection threshold', 'template similarity threshold', 'minimum ISI value', 'maximum ISI value', 'ISI distribution addition weight' and 'ISI distribution subtraction weight' were all adjusted iteratively in limited ranges and small steps until the best correlation results were produced. Unfortunately, the true positive rate was only 32.7% and false positive rate 29.3%; resulting in precision of 52.8%.

Chapter 4

Discussion and Future Work

There is potential in the far future with ENG nerve surface recording based on the theory above. However, in its current state the motions would need to be restricted, repeatable and choreographed strumming motions whilst playing guitar to manipulate audio effects post-performance. The results of my test are most likely due to small size of data to average over and reduce the impact of noise on results. Although variations in contractions force and duration may also have a large impact.

Alternatively, De Luca (2014) proposes a method which adapts to the changing shape of spikes over time. Nerve ENG as a method of tracking guitar playing in future I believe it can better reveal the intentions of the musician as it can add the dimension of force applied and variations in tension during play. The ultimate iteration would have a prototype that could automatically record and recognise common moves over time. But the signal to noise ratio and spatial resolution of wearable surface electrodes must be improved too significantly in order to use simpler, faster processing.

References

1. Gerstner, W., Kistler, W.M., Naud, R. and Paninski, L., 2014. Neuronal dynamics: From single neurons to networks and models of cognition. Cambridge University Press.
2. Franke, F., Quiroga, R.Q., Hierlemann, A. and Obermayer, K., 2015. Bayes optimal template matching for spike sorting–combining fisher discriminant analysis with optimal filtering. Journal of computational neuroscience, 38(3), pp.439-459.
3. De Luca, C.J., Chang, S.S., Roy, S.H., Kline, J.C. and Nawab, S.H., 2014. Decomposition of surface EMG signals from cyclic dynamic contractions. Journal of neurophysiology, 113(6), pp.1941-1951.
4. Sedghamiz, H. and Santonocito, D., 2015, November. Unsupervised detection and classification of motor unit action potentials in intramuscular electromyography signals. In E-Health and Bioengineering Conference (EHB), 2015 (pp. 1-6). IEEE.
5. Nenadic 2005 Spike Detection Using the Continuous Wavelet Transform
6. Choi, J. H., Jung, H. K., & Kim, T. (2006). A new action potential detector using the MTEO and its effects on spike sorting systems at low signal-to-noise ratios. IEEE Transactions on Biomedical Engineering, 53(4), 738-746
7. Zhou, W. L., Short, S. M., Rich, M. T., Oikonomou, K. D., Singh, M. B., Sterjanaj, E. V., & Antic, S. D. (2014). Branch specific and spike-order specific action potential invasion in basal, oblique, and apical dendrites of cortical pyramidal neurons. Neurophotonics, 2(2), 021006.
8. Nervous System Control Simplified. Image from: http://img.webmd.com/dtmcms/live/webmd/consumer_assets/site_images/media/medical/hw/h9991449_001.jpg
9. Cram, J. R. (2011). Cram's introduction to surface electromyography. Jones & Bartlett Learning
10. Spiegel, M. B. (1978). Electromyoneurography. American family physician, 18(5), 119-130.
11. Mika, S., Ratsch, G., Weston, J., Scholkopf, B., & Mullers, K. R. (1999, August). Fisher discriminant analysis with kernels. In Neural networks for signal processing IX, 1999. Proceedings of the 1999 IEEE signal processing society workshop. (pp. 41-48). Ieee.
12. Harris, Kenneth D., Darrell A. Henze, Jozsef Csicsvari, Hajime Hirase, and Gyorgy Buzsaki. "Accuracy of tetrode spike separation as determined by simultaneous intracellular and extracellular measurements." Journal of neurophysiology 84, no. 1 (2000): 401-414. Bankman, I. N., Johnson, K. O., & Schneider, W. (1993). Optimal detection, classification, and superposition resolution in neural waveform recordings. IEEE transactions on biomedical engineering, 40(8), 836-841
13.Yang, Xiaowei, and Shihab A. Shamma. "A totally automated system for the detection and classification of neural spikes." IEEE Transactions on Biomedical Engineering 35, no. 10 (1988): 806-816.

14. Oweiss, K. G. (2002). Multiresolution analysis of multichannel neural recordings in the context of signal detection, estimation, classification and noise suppression (Doctoral dissertation).
15. Purves, D., G. J. Augustine, D. Fitzpatrick, L. C. Katz, A. S. LaMantia, J. O. McNamara, and S. M. Williams. "Increased conduction velocity as a result of myelination." Neuroscience(2001).
16. Trigno EMG System User Guide. Website last accessed 03/08/2018: https://delsys.com/Attachments_pdf/download/users-guides/trigno-im.pdf.
17.Lähdeoja, O. (2010). La guitare électrique augmentée: cadre de travail et stratégies pour la conception d'un instrument augmenté. Appareil, (5).
18.Waksman, S. (2001). Instruments of desire: The electric guitar and the shaping of musical experience. Harvard University Press.
19. Carfoot, G. (2006). Acoustic, electric and virtual noise: The cultural identity of the guitar. Leonardo music journal, 35-39.
20.Thompson, W. (2015).Music, thought and feeling. Understandiing the psychology of music.Oxford University Press

Appendix A: Input ENG Nerve Data after Upsampling and Bandpass.

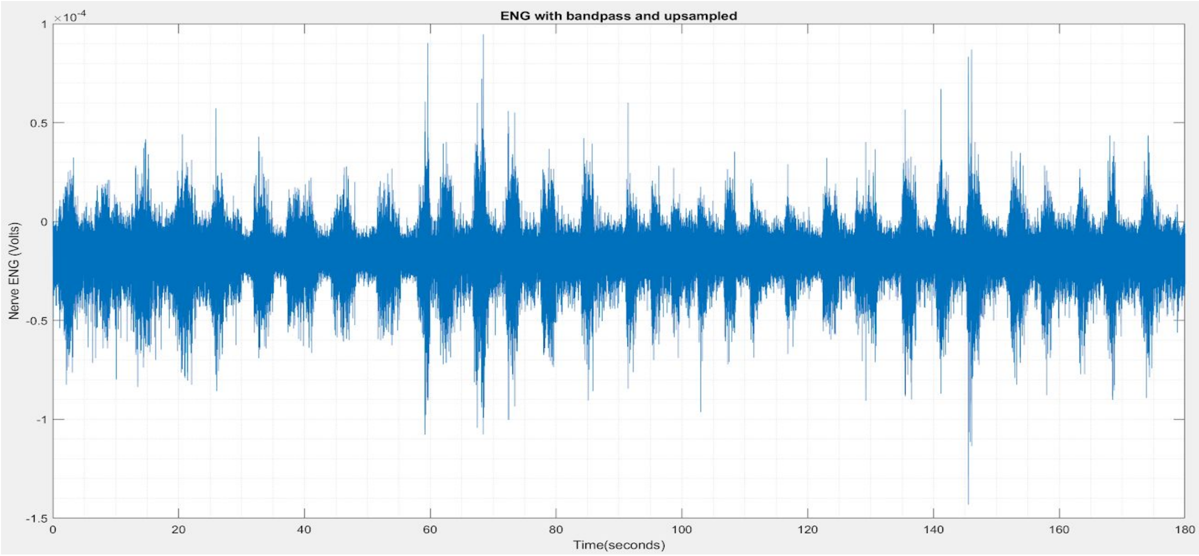

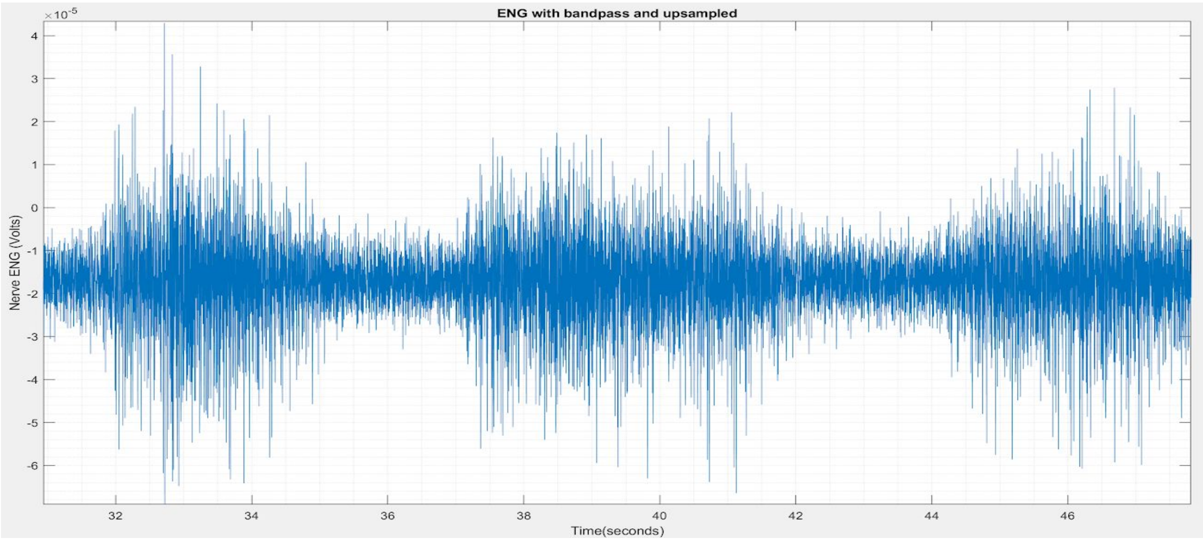

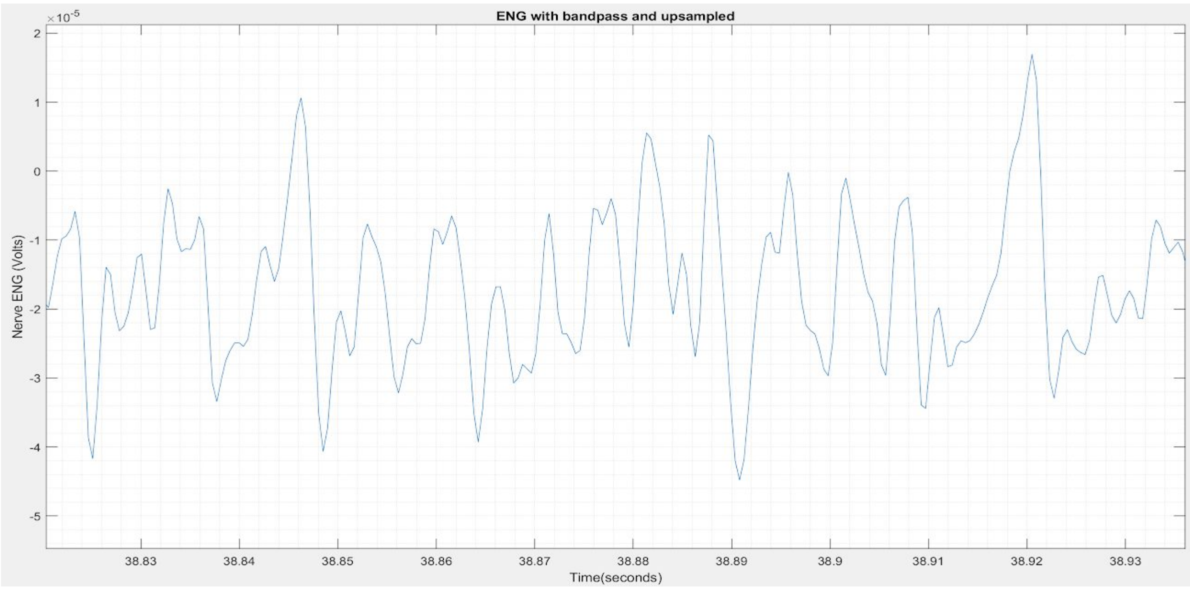

Appendix B: RMS Muscle Activity coloured per mass (Top), 3-axis Accelerometer (Middle) and Contraction Time Windows with sorted spikes per neuron (Bottom).

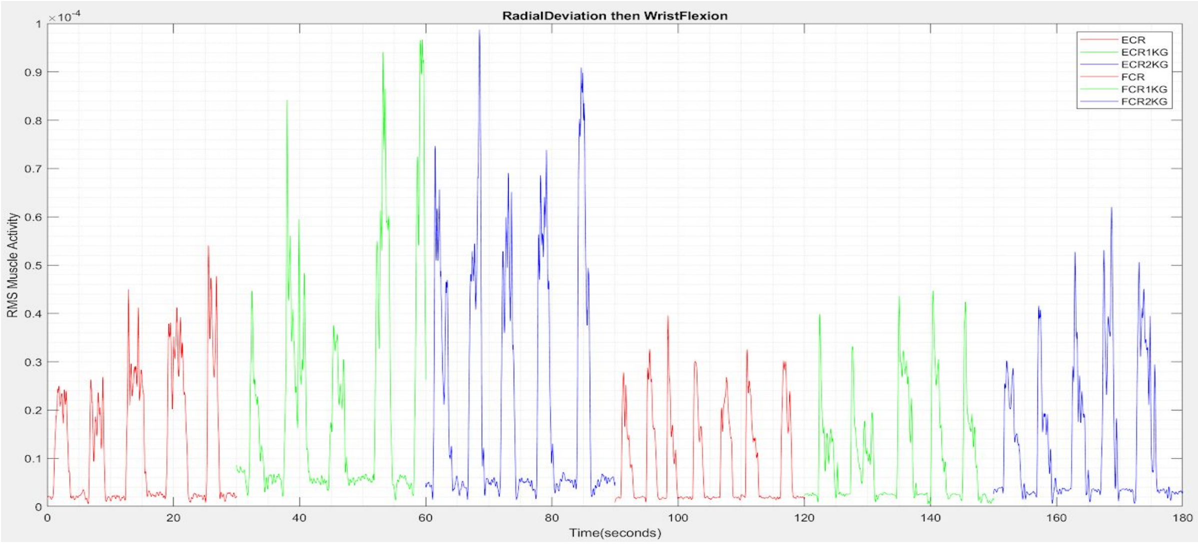

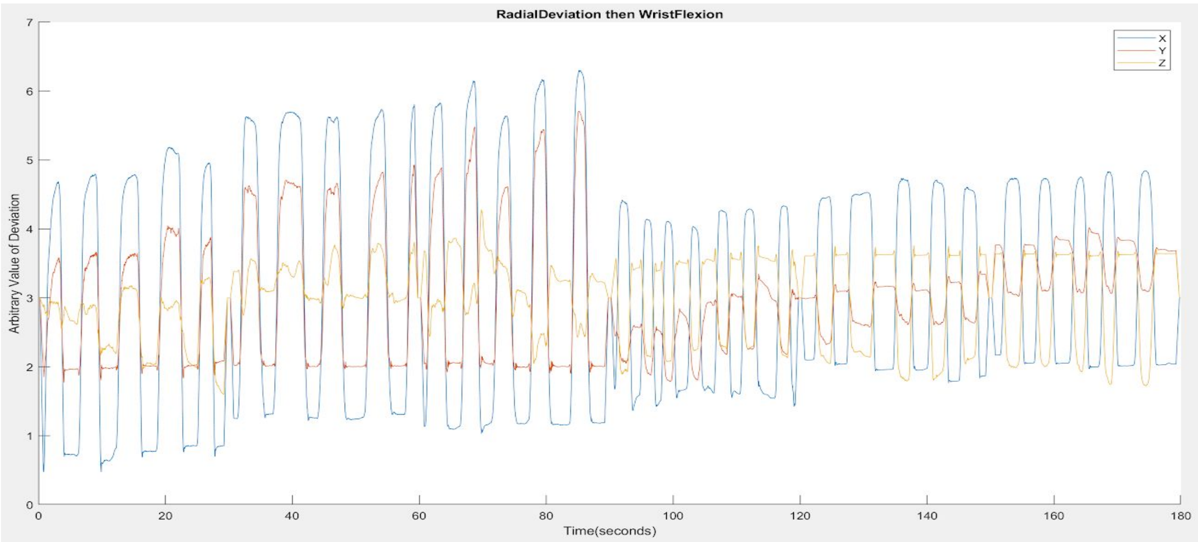

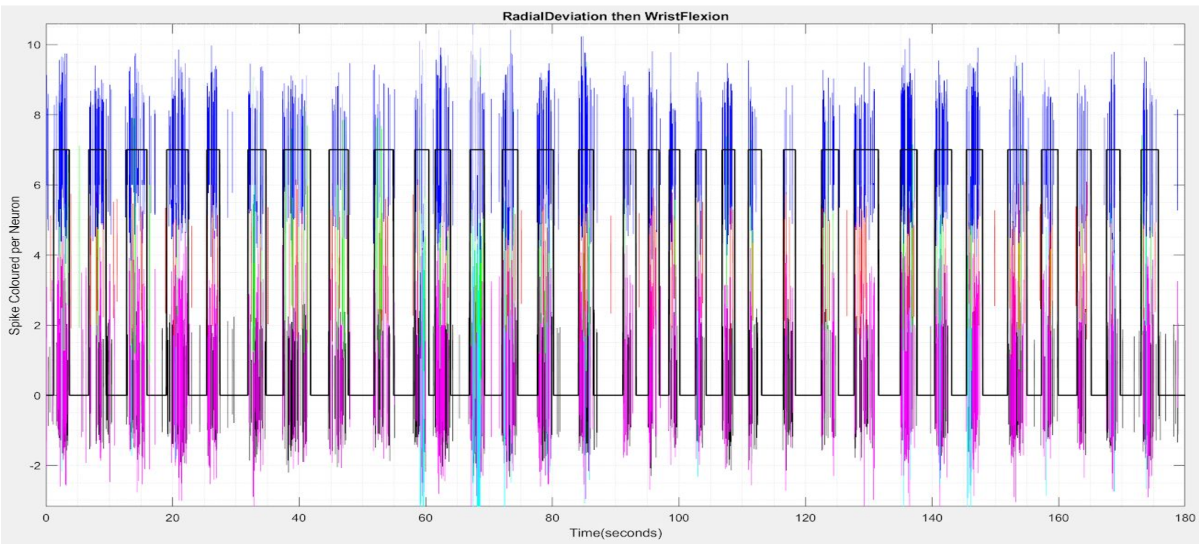

Appendix C: Detected Spikes with Templates coloured per Neuron over time with contraction windows (solid black line).

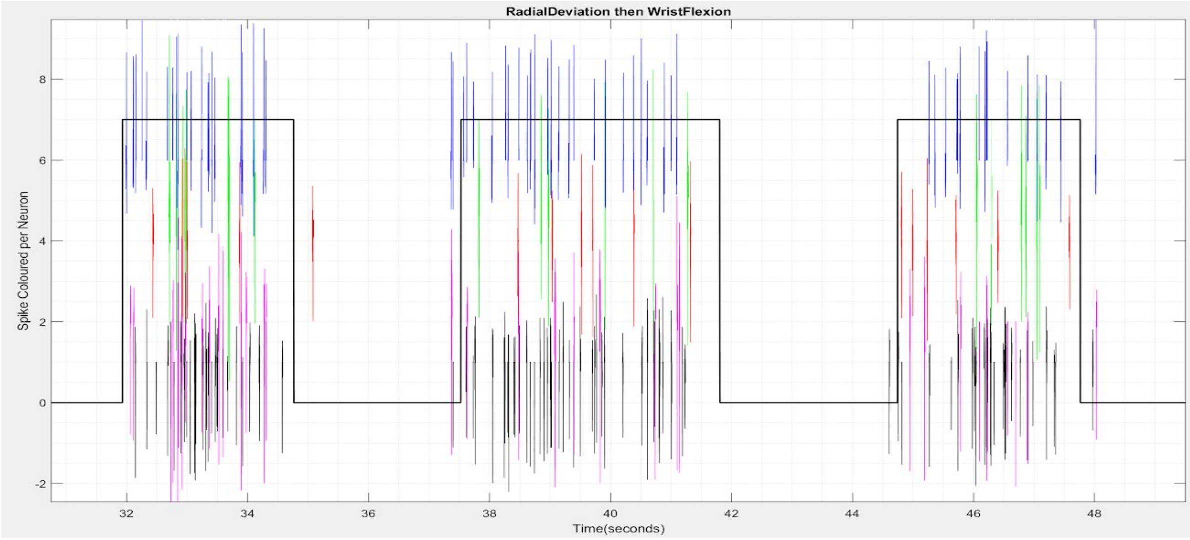

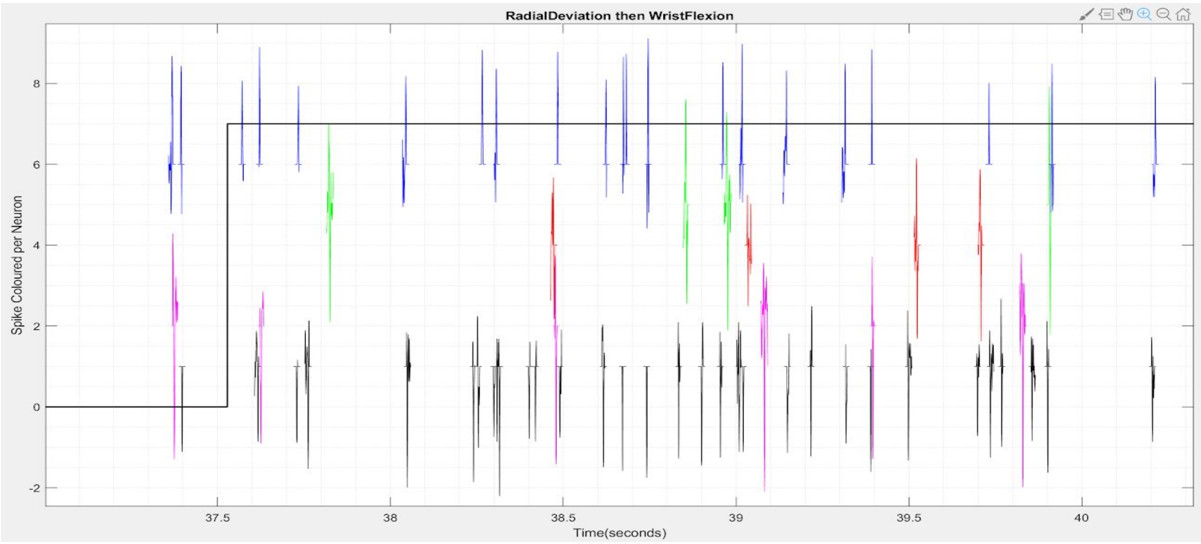

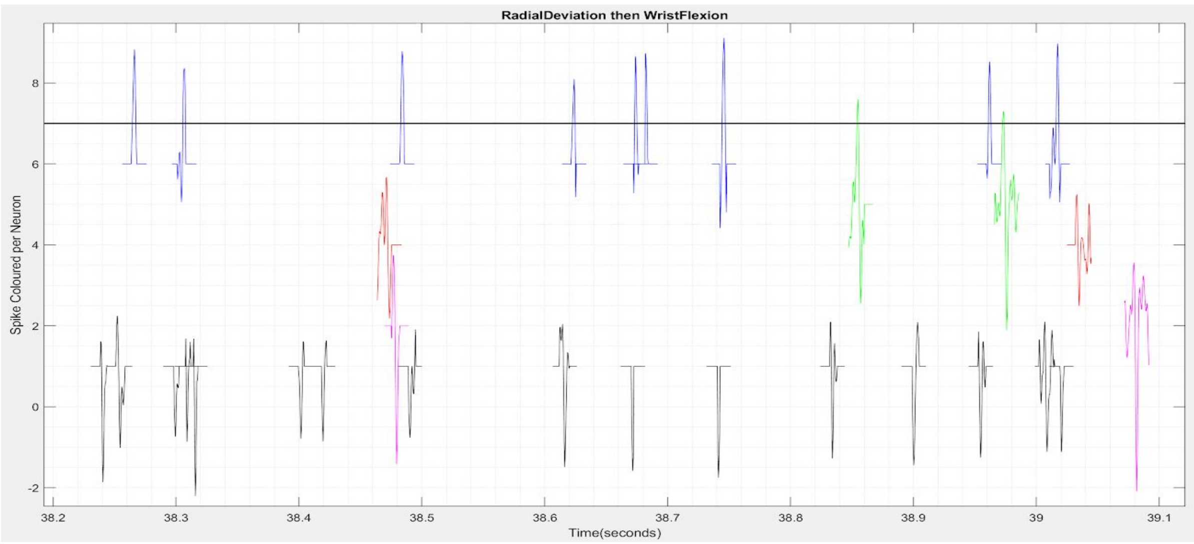

Appendix D: Interspike Interval Distributions per Label (Training data in blue, Randomly selected test data in red).

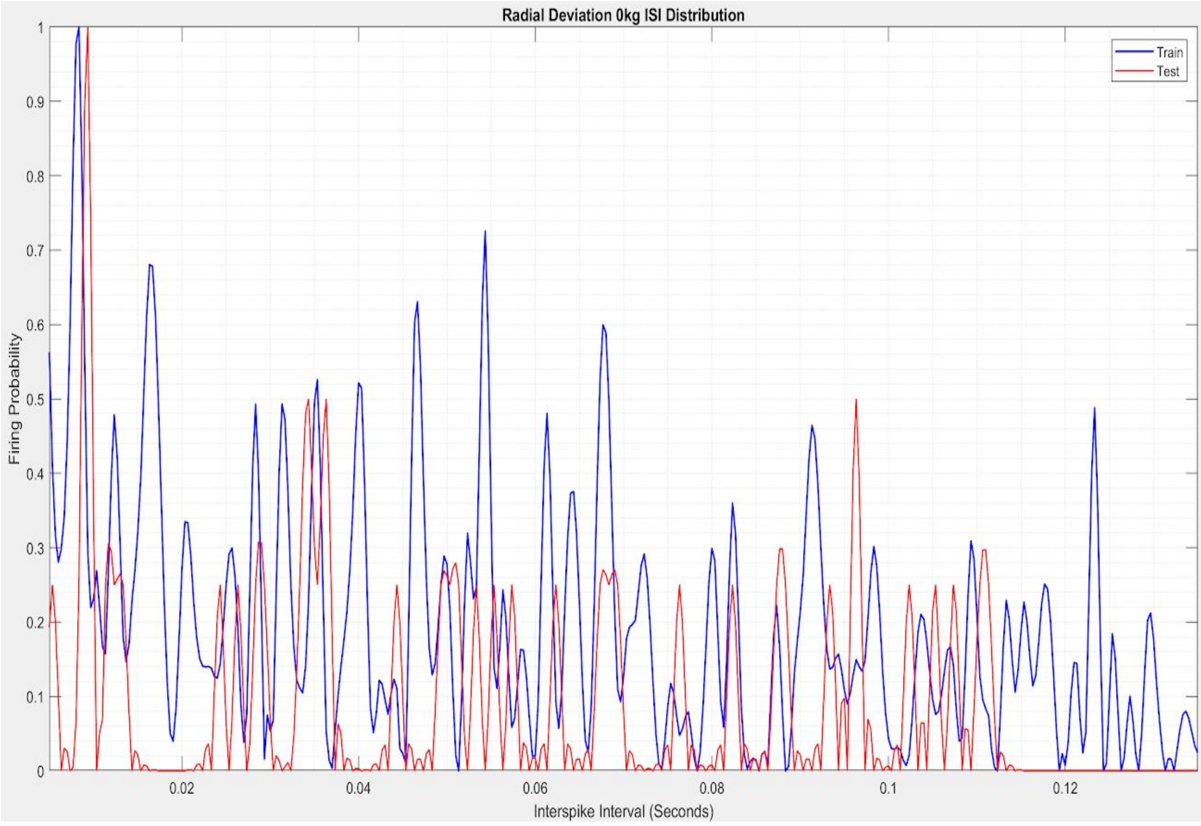

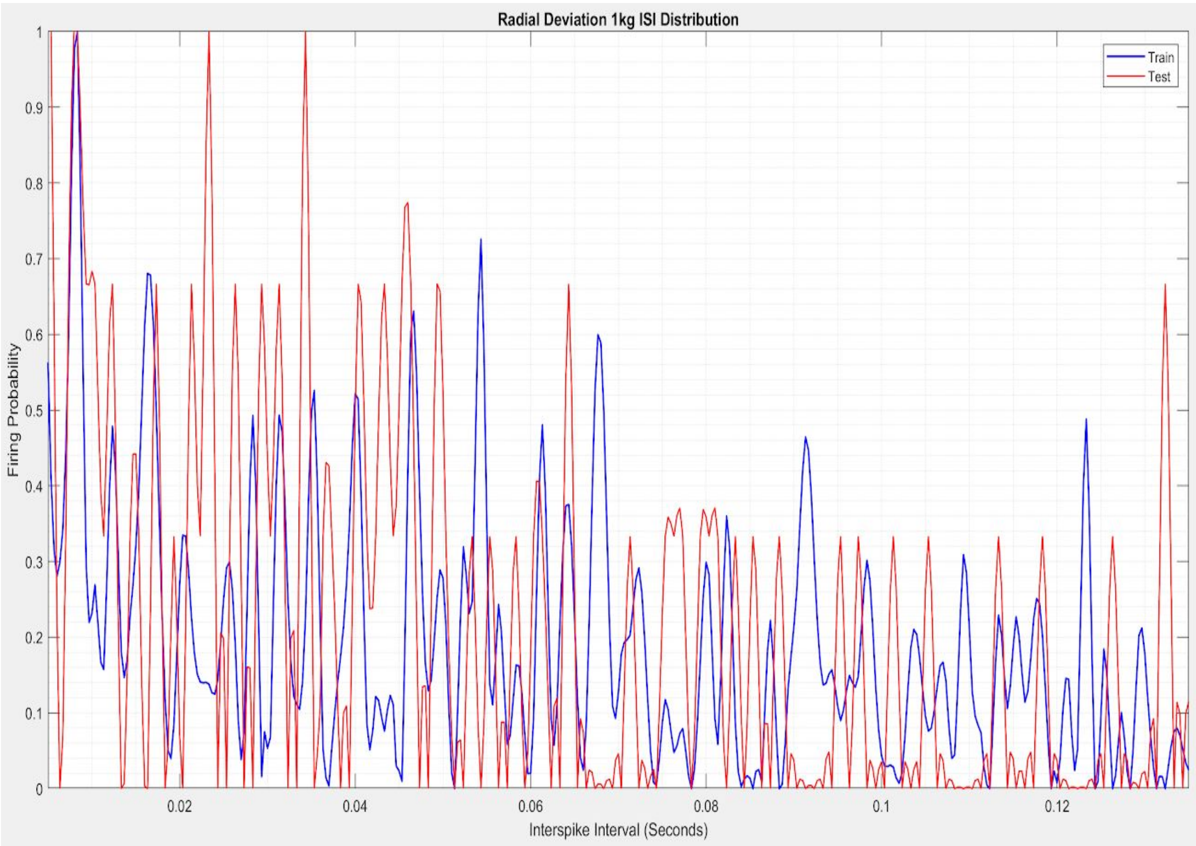

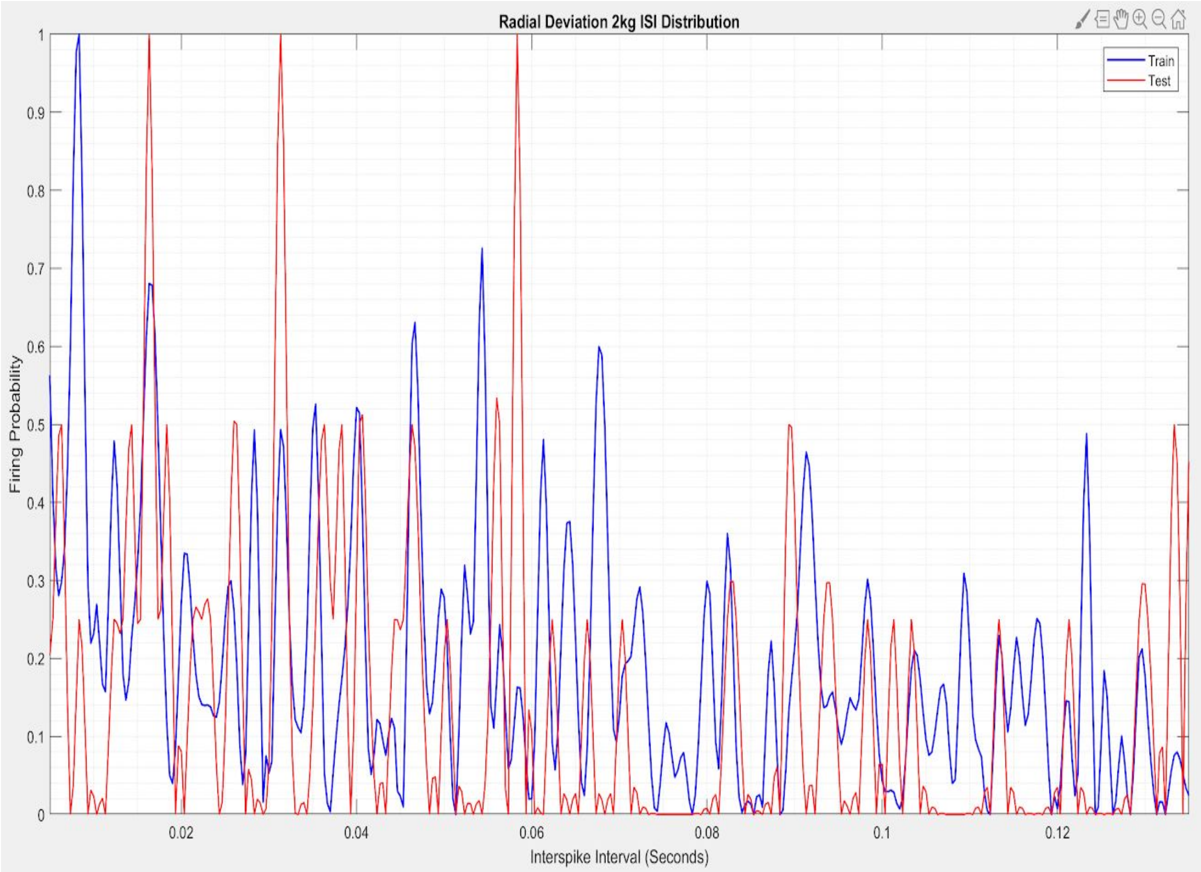
Radial Deviation 2kg ISI Distribution
Train
Test
Firing Probability
Interspike Interval (Seconds)
0
0.1
0.2
0.3
0.4
0.5
0.6
0.7
0.8
0.9
1
0.02
0.04
0.06
0.08
0.1
0.12

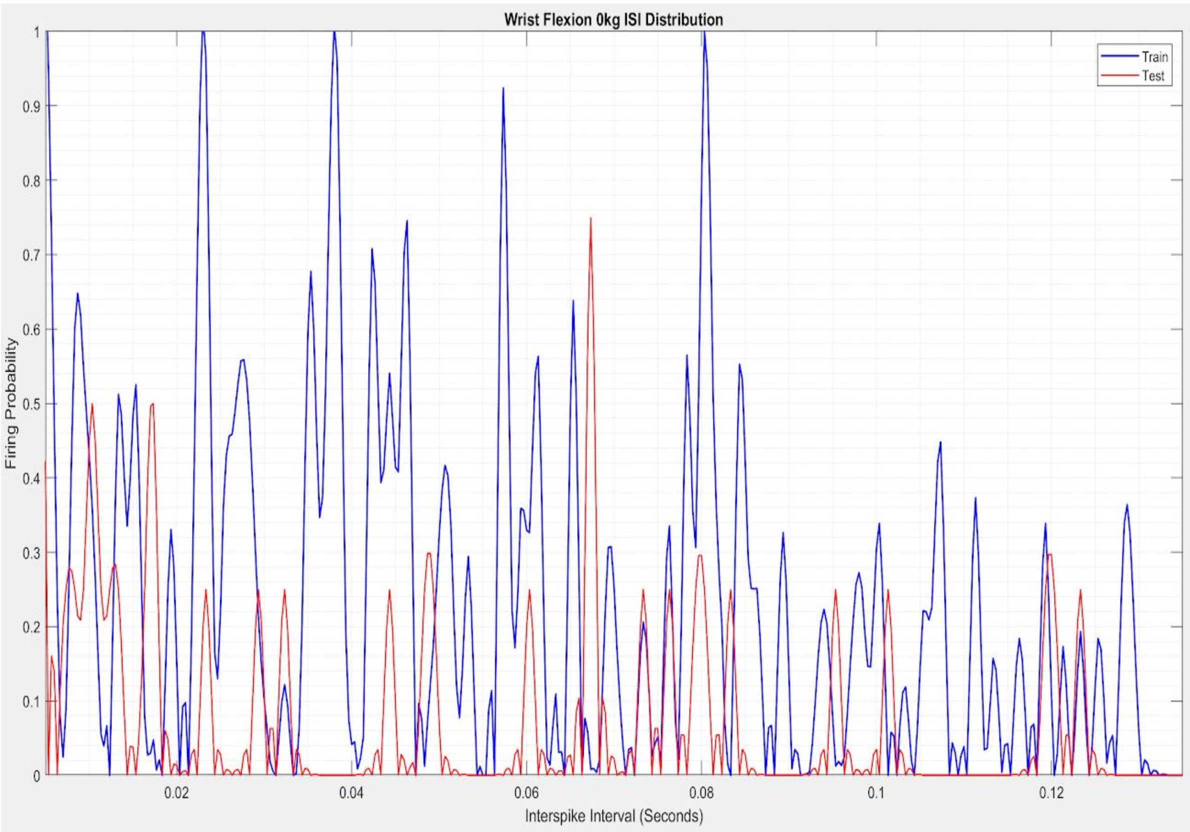
Wrist Flexion 0kg ISI Distribution
Train
Test
Firing Probability
Interspike Interval (Seconds)
0
0.1
0.2
0.3
0.4
0.5
0.6
0.7
0.8
0.9
1
0.02
0.04
0.06
0.08
0.1
0.12

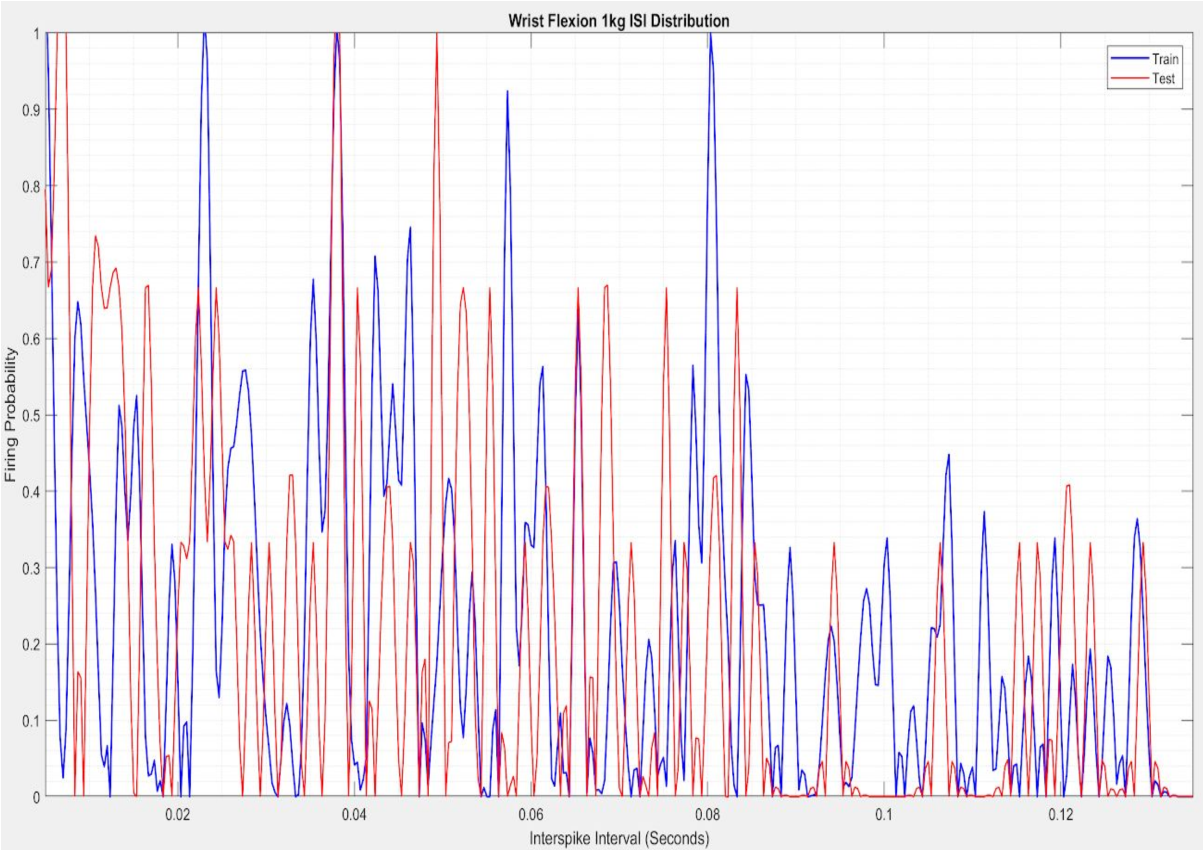

Wrist Flexion 1kg ISI Distribution
Train
Test
Firing Probability
Interspike Interval (Seconds)

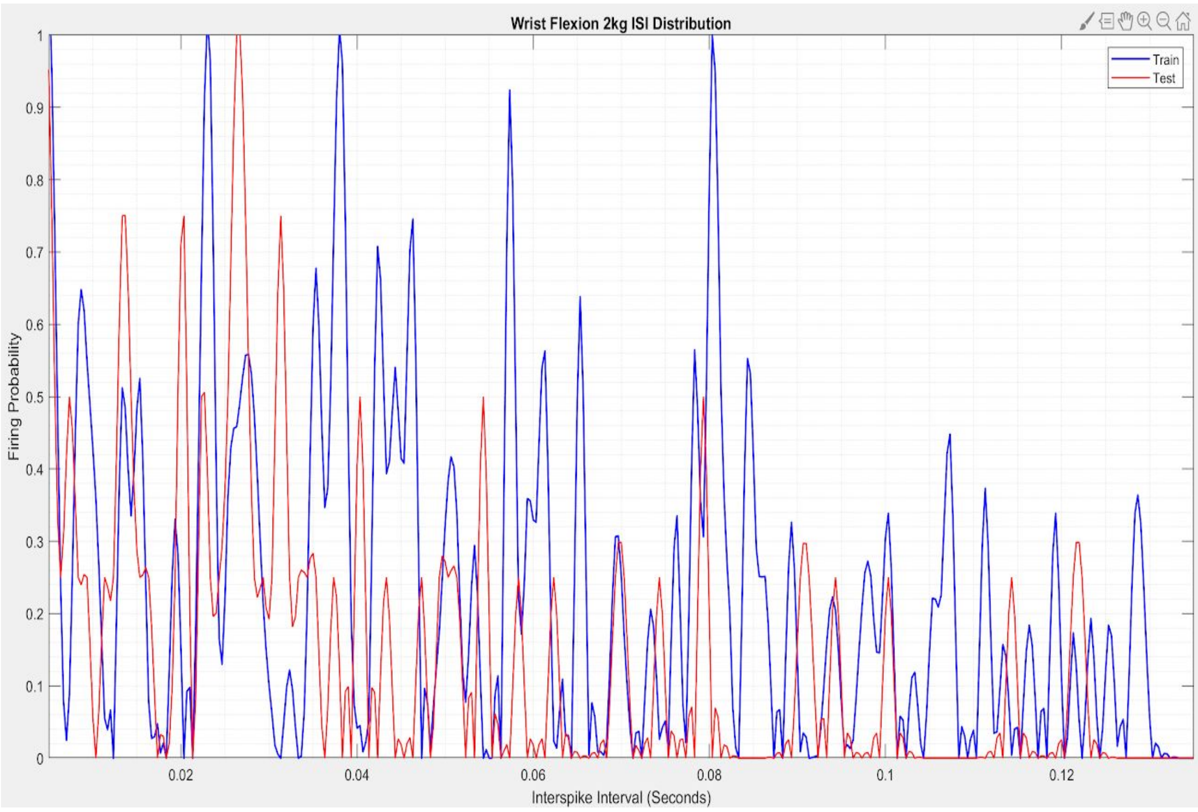

Wrist Flexion 2kg ISI Distribution
Train
Test
Firing Probability
Interspike Interval (Seconds)

Appendix E: ISI Distribution Cross Correlation Results using cross-validation.

Each figure represents the correlation results for the five contractions from the label marked on the title of the figure (Median=red line, Quantiles=Blue box, Outliers=Red cross and Minimum and Maximum=black lines)

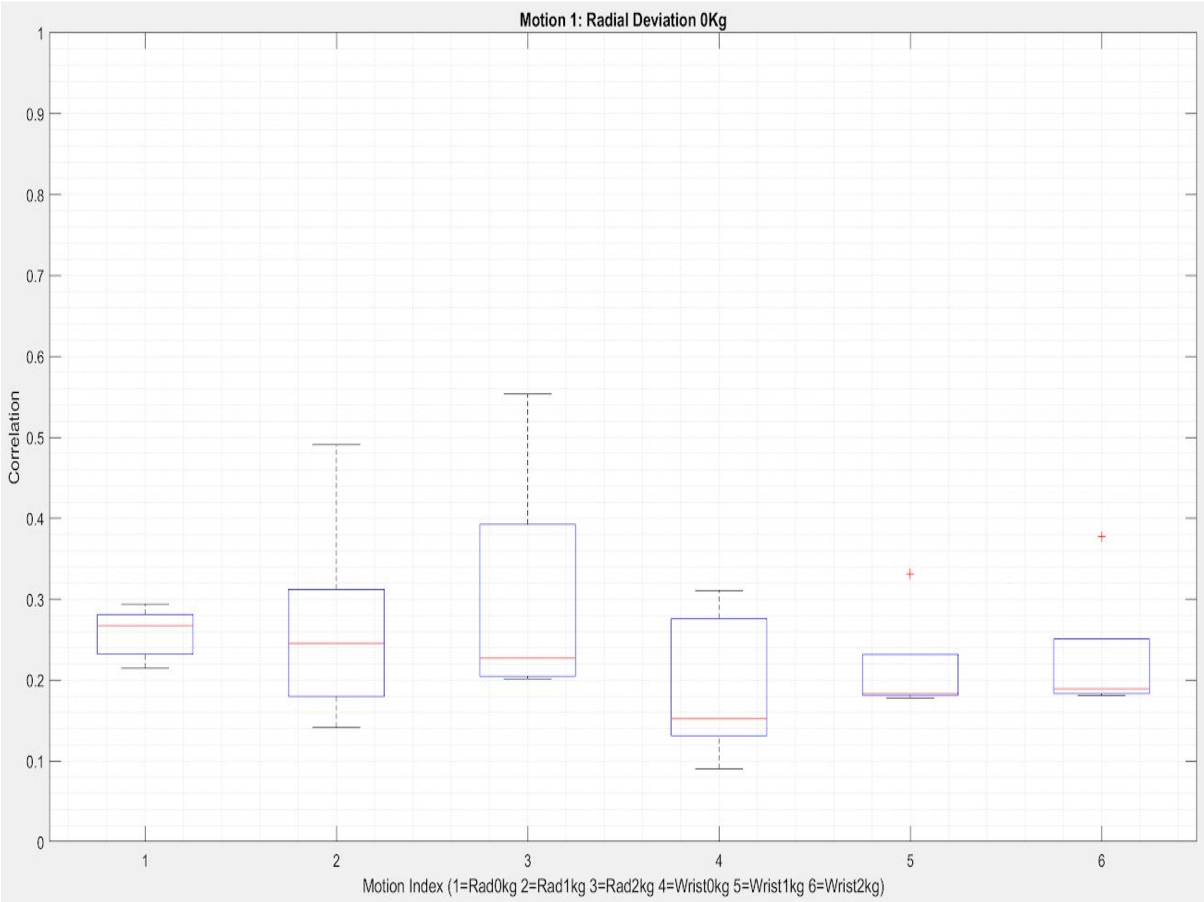

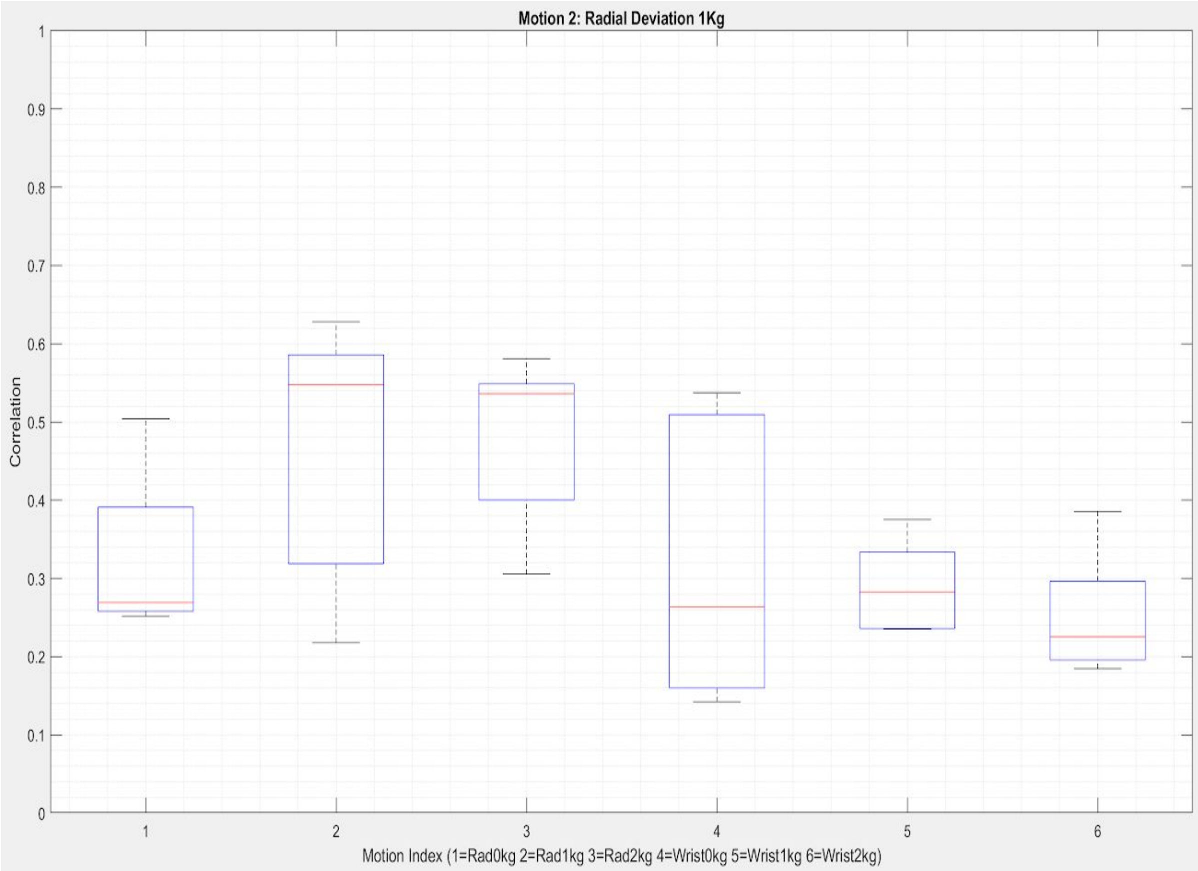
Motion 2: Radial Deviation 1Kg
Correlation
Motion Index (1=Rad0kg 2=Rad1kg 3=Rad2kg 4=Wrist0kg 5=Wrist1kg 6=Wrist2kg)

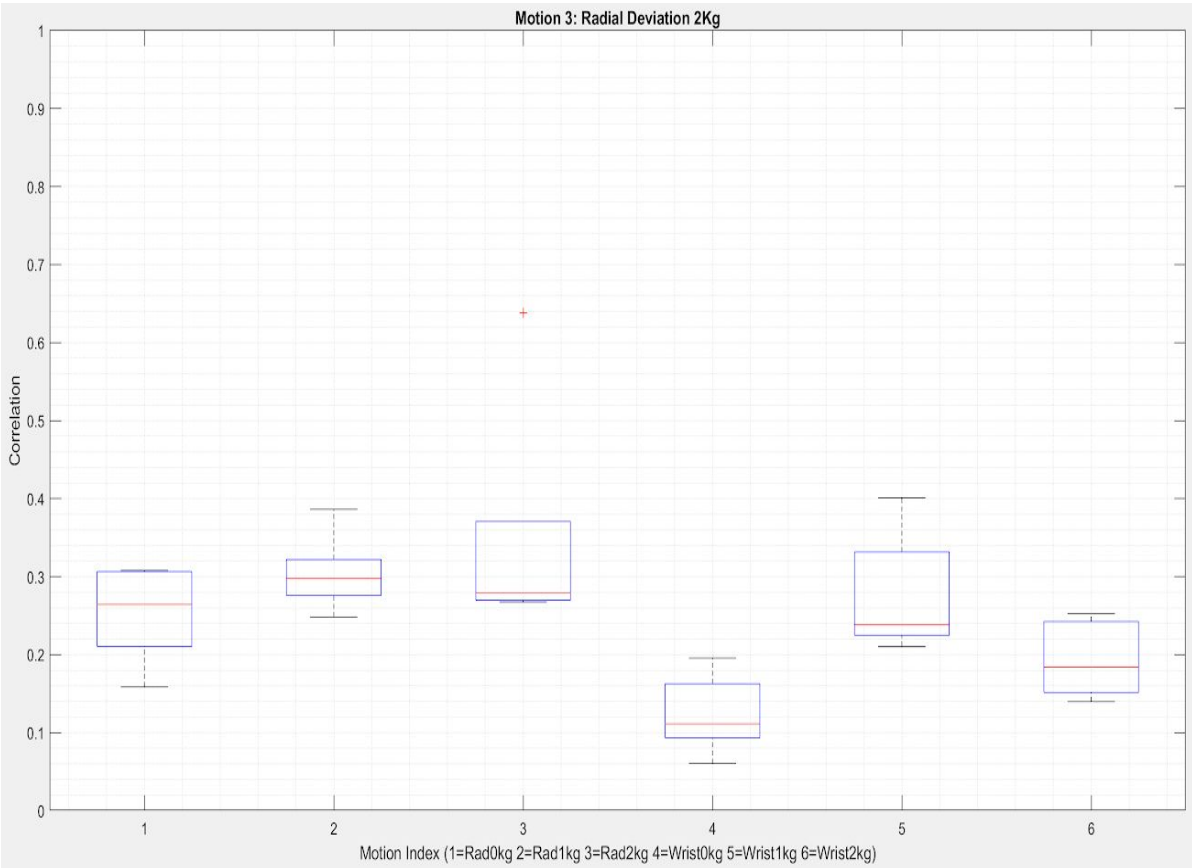
Motion 3: Radial Deviation 2Kg
Correlation
Motion Index (1=Rad0kg 2=Rad1kg 3=Rad2kg 4=Wrist0kg 5=Wrist1kg 6=Wrist2kg)

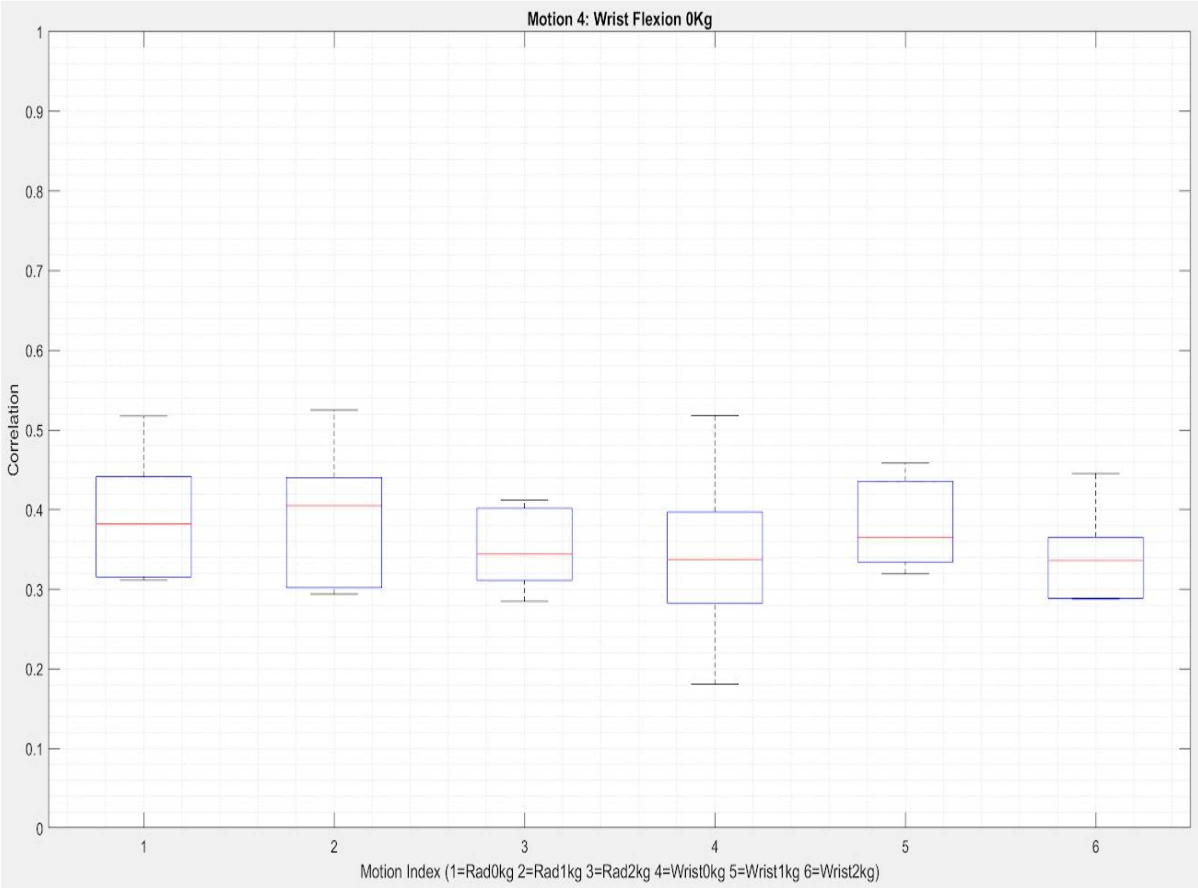

Motion 4: Wrist Flexion 0Kg
Correlation
1
0.9
0.8
0.7
0.6
0.5
0.4
0.3
0.2
0.1
0
1
2
3
4
5
6
Motion Index (1=Rad0kg 2=Rad1kg 3=Rad2kg 4=Wrist0kg 5=Wrist1kg 6=Wrist2kg)

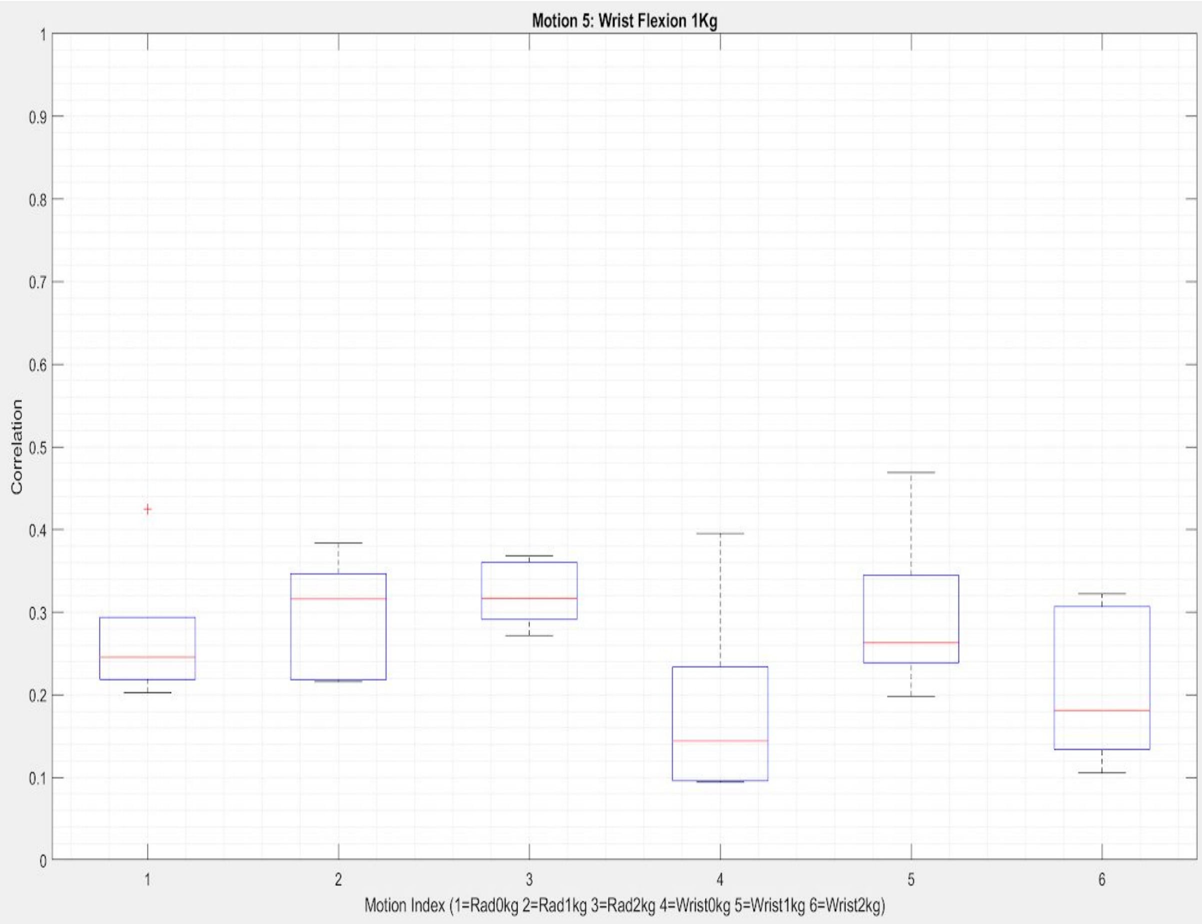
Motion 5: Wrist Flexion 1Kg
Correlation
Motion Index (1=Rad0kg 2=Rad1kg 3=Rad2kg 4=Wrist0kg 5=Wrist1kg 6=Wrist2kg)

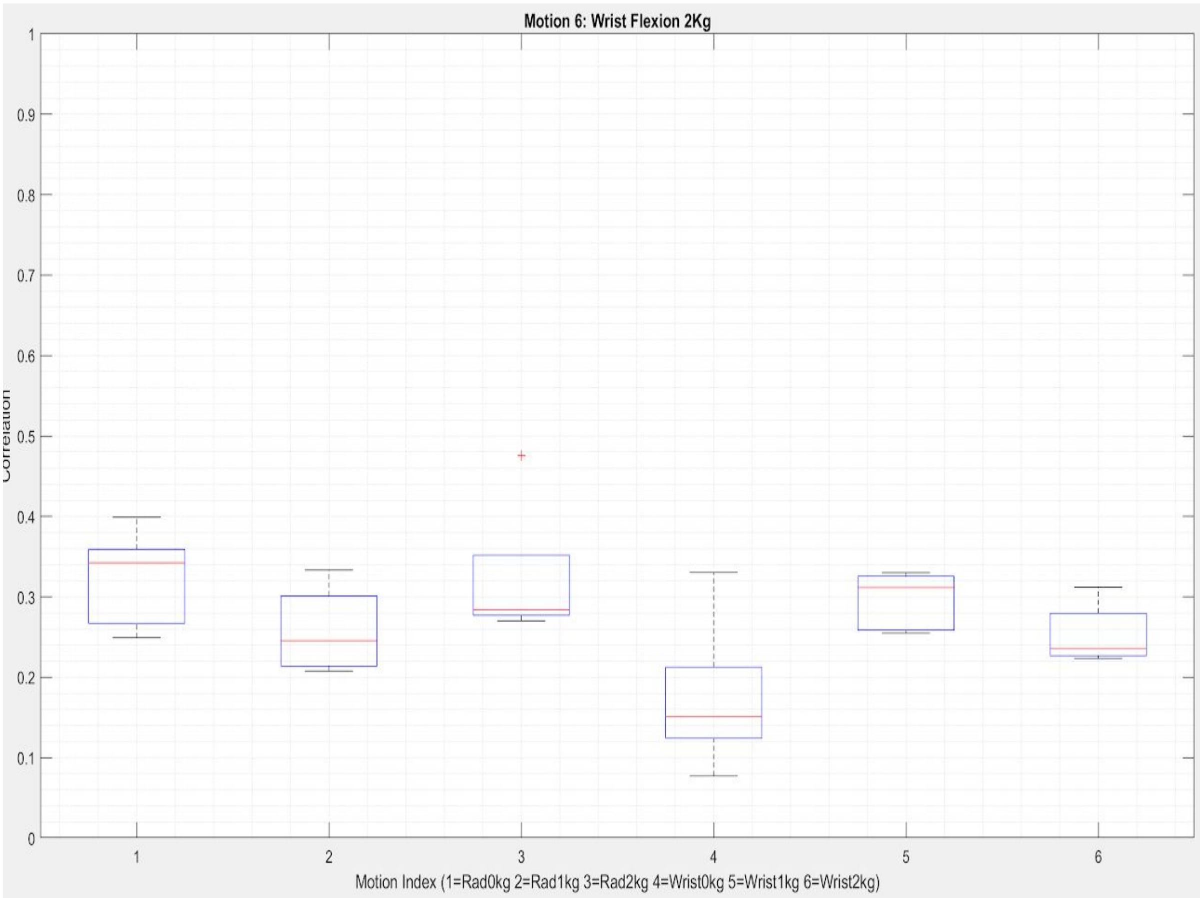
Motion 6: Wrist Flexion 2Kg
Correlation
Motion Index (1=Rad0kg 2=Rad1kg 3=Rad2kg 4=Wrist0kg 5=Wrist1kg 6=Wrist2kg)